NTNU – Trondheim
Norwegian University of
Science and Technology

Surface Modified γ-Alumina Supports For Cobalt Fischer-Tropsch Catalysts

Ata ul Rauf Salman

Chemical Engineering
Submission date: July 2015
Supervisor: Magnus Rønning, IKP
Co-supervisor: Anders Holmen, IKP
Erling Rytter, IKP
Nikolaos Tsakoumis, IKP

Norwegian University of Science and Technology
Department of Chemical Engineering

Dedicated to Nature,
its Creator and,
My Parents

Acknowledgement

Foremost, I would like to express my profound gratitude to my supervisor, **Magnus Rønning** for his exceptional supervision, valuable research guidance and continuous support at every stage of the project. My sincere thanks goes to him for introducing me to catalysis field by offering me the summer internship opportunity.

I would like to extend my whole-hearted thanks to my supervisor **Nikolaos Tsakoumis** for his motivation, encouragement and unparallel support in every field, whether it's experimental work, results analysis or writing at all levels of the project.

Thanks a lot to my advisors **Rune Myrstad**, **Erling Rytter** and **Anders Holmen** for enlightening me with their immense knowledge, insightful comments and valuable suggestions at various stages of the project.

I would also like to thank **Jia yang** for teaching me all the fundamental techniques of catalysis which enabled me to carry out this research work. This small endeavor would not have been realised without all help from all these people.

My deepest gratitude for my **parents** for their endless love, support & encouragement and who have been the pillars of my success in all that I have achieved so far.

I do extend my sincere thanks to **Sulalit Bandyopadhyay** (PhD at Dept. of Chemical Engineering, NTNU) for his support, suggestion and help throughout the course of work.

Finally, I must thank **God** for bestowing upon me his blessing and giving me the strength for making this attempt a fruitful one.

Abstract

Fischer-Tropsch synthesis over cobalt based catalysts is an important route for the conversion of syngas, derived from natural gas, to liquid fuels. Fischer-Tropsch performance of cobalt catalysts depends on a number of factors, for instance the type and structure of support have a significant effect on the particle size, dispersion, reducibility. These, in turn, affect the activity of the cobalt supported catalysts [1–4]. Silica supports surface modified with different silanes, have been studied for cobalt Fischer-Tropsch synthesis [5–8]. Modification of γ-Al_2O_3 with silanes to yield hydrophobic surfaces has been carried out [9–11]. However, use of silane modified γ-Al_2O_3 as a support for cobalt Fischer-Tropsch synthesis has not been studied until now.

Herein, a systematic study was performed to investigate the effect of silane modification on activity and selectivity of γ-Al_2O_3 supported cobalt Fischer-Tropsch catalysts. Six silane modified Co/γ-Al_2O_3 catalysts were prepared by organic phase silylation with various silanes differing with respect to number and type of active and organic groups. Catalysts with 20 wt % Co promoted with 0.5 wt % Re were prepared by one step aqueous incipient wetness impregnation. Catalysts were characterized by H_2 chemisorption, N_2 adsorption, temperature programmed reduction (TPR), thermal gravimetric analysis (TGA), Fourier transform infra-red spectroscopy (FT-IR) and X-ray diffraction (XRD). Activity and selectivity of catalysts was determined in a fixed bed reactor at 20 bar, 210 ^oC and H_2/CO = 2.1.

Effective surface organic modification of support was indicated by water absorption and FT-IR. Most promising results in terms of Fischer-Tropsch activity and selectivity, were displayed by methoxytrimethylsilane (TMMeS) modified catalyst. H_2 chemisorption, XRD and TPR revealed enhanced dispersion, similar cobalt crystallite size and reducibility as reference catalyst. TG suggested partial decomposition below calcination temperature. Site-time yield (STY) increased to 0.071 s^{-1} and C_{5+} selectivity slightly decreased to 85.15 % in comparison with 0.064 s^{-1} and 85.69 % of reference catalyst respectively.

Chlorotrimethylsilane, dichlorodimethylsilane and chlorodimethyloctylsilane modified catalysts had lower cobalt crystallite sizes than the reference catalyst. A positive correlation was observed between crystallite sizes and amount of silane present. Despite of smaller cobalt crystallite size, modified catalysts have similar reducibility attributed to lower cobalt support interaction as a result of surface modification. Dispersion measured from hydrogen chemisorption was apparently lower than actual. Smaller cobalt crystallite and lower dispersion were ascribed to presence of chlorine and it needs further investigation. Relatively small changes were observed in C_{5+} selectivity but STY decreased significantly.

Catalyst modified with methoxydimethyoctylsilane exhibited similar cobalt crystallite size and observed a similar increase in STY to 0.071 s^{-1} as TMMeS modified catalyst but C_{5+} selectivity decreased to 83.04 % in comparison with reference catalyst. Modification with trichloroctylsilane had the most severe impact with STY decreasing to 0.02 s^{-1}.

The results indicate a positive effect of methoxy-silanes modification on the activity of catalysts, ascribed to hydrophobicity induced by surface modification. Effect of chlorosilane on dispersion, cobalt crystallite size and activity of catalysts need further investigation.

Table of Contents

List of Tables

List of Figures

Abbreviations

A	Ampere
ASF	Anderson-Schulz-Flory
ATR	Attenuated total reflection
BET	Brunauer-Emmett-Teller
CNG	Compressed natural gas
D	Dispersion
DMDCS	Dichlorodimethylsilane
DMDES	Dimethyldiethoxysilane
DMMeOS	Methoxydimethyloctylsilane
DMOCS	Chlorodimethyloctylsilane
ECD	Electron capture detector
FID	Flame ionisation detector
FT	Fischer-Tropsch
FT-IR	Fourier transform infra-red spectroscopy
GC	Gas chromatography
GTL	Gas to liquid
HTFT	High temperature Fischer-Tropsch
IR	Infra-red
LNG	Liquefied natural gas
LTFT	Low temperature Fischer-Tropsch
MS	Mass spectrometer
MTES	Methyltriethoxysilane
OTCS	Trichloroctylsilane
Po	Post-modified
Pr	Pre-modified
STY	Site-time yield
Syngas	Synthesis gas
TCD	Thermal conductivity detector
TGA	Thermal gravimetric analysis
TMCS	Chlorotrimethylsilane
TMMeS	Trimethylmethoxysilane
TOF	Turn over frequency
TPR	Temperature programmed reduction
WGS	Water gas shift
XRD	X-ray diffraction

Symbols

α	Probability of chain growth
β	Line broadening
λ	Wavelength of the X-rays
θ	Angle between the incident X-rays and normal
A_M	Concentration of the component A in mobile phase
A_S	Concentration of the component A in stationary phase
$a.u$	Arbitrary unit
d_v	Volume-weighted crystallite diameter
K_c	distribution constant
V_{imp}	Impregnating liquid volume
V_p	Support pore volume
a_m	surface area occupied by a metal atom
c	constant in BET
Co/γ-Al_2O_3	Referenc Catalyst
Co/(γ-Al_2O_3)$_{Po1}$	DMMeOS post-modified catalyst
Co/(γ-Al_2O_3)$_{Po2}$	OTCS post-modified catalyst
Co/(γ-Al_2O_3)$_{Pr1}$	TMMeS pre-modified catalyst
Co/(γ-Al_2O_3)$_{Pr2}$	TMCS pre-modified catalyst
Co/(γ-Al_2O_3)$_{Pr3}$	DMDCS pre-modified catalyst
Co/(γ-Al_2O_3)$_{Pr4}$	DMOCS pre-modified catalyst
d	Lattice spacing
K	Constant
m	Mass
M	Atomic mass of the metal
M_s	Surface metal atom
N_A	Avogadro's number
p	Pressure of the gas
p_0	Saturated vapour pressure
r_p	Rate of polymerization
r_t	Rate of termination
V	Volume of the adsorbed gas
v_m	Molar volume
V_m	Volume equivalent to an adorbed monolayer
w_m	Weight fraction of active metal
x_n	Molar fraction of each carbon number

Chapter 1

Introduction

From the early history of mankind to the current advanced technological world, the sources of energy have evolved gradually. In early times, the energy needs were quite simple and were fulfilled with wood and biomass, mostly for heating and cooking purposes. Industrial revolution of the 18th century was attributed to the use of coal mostly in steam engines and power plants. In the 19th century, coal was gradually replaced with oil. The consumption of fossil fuels increased exponentially with advancement in transportation and production industries. Today world economy depends to a large extent on fossil fuels derived petroleum fractions i.e gasoline, diesel and natural gas.

The global energy demand is anticipated to increase by 35% in 2040 as compared to 2010 and global economy will be almost doubled over the same period of time [12]. The increase in energy demand turns out to be associated with population growth and consumption of energy per capita. It is increasing at an exponential rate and is projected to increase from 7 billion in 2010 to 9 billion in 2040 [12].

To meet the increasing world's energy demand is the biggest challenge. Fossil fuels are non-renewable and their resources are depleting continuously. It is of utmost importance to find alternate energy sources. Extensive research is being carried out for several potential renewable energy sources. Biomass, wind energy and solar energy are of significant importance.

Huge resources of natural gas exist which are estimated to last for 200 years at the current yearly consumption rate [12]. Natural gas is expected to become future fuel due to its availability, efficiency and clean burning properties. Natural gas can play a vital role in meeting world energy demands. Resources of natural gas are quite diverse and distributed across the world in contrast with the other fossil fuels. Natural gas can also be produced from unconventional resources like shale gas and tight gas [12].

Huge investments are required to shift from liquid fuel based infrastructure to gas based. Gaseous phase of natural gas also poses difficulties during transportation. It can either be transported in compressed form (CNG) compressed natural gas, liquefied form; liquefied natural gas (LNG) or can be converted to liquid chemicals. Fischer-Tropsch enables conversion of natural to liquid fuels and the products obtained have high purity

and are virtually free from sulphur and nitrogen containing compounds thus helping in resolving increased environmental concerns. Coal and natural gas are the most important feed stocks.

Currently one of the most important interest is the consideration of Fischer-Tropsch synthesis to the flared natural gas at certain huge oil fields having high levels of natural gas[13]. This can resolve environmental issues as well as increase profitability. Interest in use of bio-mass as feed stock for Fischer-Tropsch is also increasing [14].

Fischer-Tropsch synthesis aims at converting synthesis gas, derived from natural gas, coal or other carbonaceous feed stocks, catalytically into higher hydrocarbons. Product selectivity of C_5+ hydrocarbons is used as a measure of production of higher hydrocarbons. Cobalt based supported catalysts are mostly used for conversion of natural gas based synthesis gas to liquid fuels [15]. Enormous research has been carried out and several factors i.e temperature, pressure, syngas composition and type of active metal used, have been identified in a quest to increase the activity and selectivity of the catalyst. The purity, structure and type of support, the synthesis variables such as cobalt precursor and solvent, preparation method, cobalt loading, pretreatment conditions (drying, calcination, reduction) and promoters have an influence on particle size, dispersion and reducibility and hence the activity & selectivity to higher (C_5+) hydrocarbons [15].

Cobalt Fischer-Tropsch catalysts are mostly supported on SiO_2, Al_2O_3, TiO_2.[16, 17]. Catalytic properties of cobalt based catalyst are influenced by the support material used. Reducibility and dispersion of cobalt catalyst are influenced by the texture and surface properties of support [18, 19]. The type and structure of support have a significant effect on the particle size, dispersion, reducibility which thus affects the activity of the cobalt supported catalysts [1–4, 16, 20–27].
Support material used also influences the product distribution in Fischer-Tropsch synthesis. For instance use of different alumina phases lead to different selectivities for C_5+ ranging in the order Co/α-Al_2O_3 > Co/δ-Al_2O_3 > Co/θ-Al_2O_3 > Co/γ-Al_2O_3 [28].

1.1 Goal

The overall goal of this research work was to the investigate the effect of silane modification on activity & selectivity of Co/γ-Al_2O_3 Fischer-Tropsch catalyst.

Silica supports modified with different silanes have been studied for cobalt Fischer-Tropsch synthesis and reported to have a positive influence on C5+ selectivity [5–8]. Successful modification of γ-Al_2O_3 with silanes to yield hydrophobic surfaces has been reported [9–11]. However use of silane modified γ-Al_2O_3 as support for cobalt Fischer-Tropsch synthesis has not been studied until now. Silane modification has two fold advantage as two effects can be studied simultaneously

1. Effect of hydrophobic nature of catalyst as water affects the activity and selectivity of Co/γ-Al_2O_3 [26, 29].

2. Effect of concentration of surface hydroxyl groups. The difference in higher hydrocarbon (C_{5+}) selectivity of different transitional aluminas is postulated to be due to difference in chemical properties [30].

One of the main differences between surface of α-Al_2O_3 and γ-Al_2O_3 is the amount of hydroxyl groups with γ-Al_2O_3 having higher number. Substitution of surface hydroxyl groups of γ-Al_2O_3 with silane will help in understanding the effect of hydroxyl groups.

1.2 Strategy

Ample hydroxyl groups on the surface of γ-Al_2O_3 were exploited and substituted by chemical reaction with silane resulting in hydrophobic surface and altered surface properties. Six different silanes were used for liquid phase (non-aqueous) surface modification of γ-Al_2O_3. Silanes used have the general formula $\mathbf{R}_n$**-Si-**$\mathbf{X}_{4-n}$ where

- n = 3
- R = methyl-, octyl-
- X = methoxy-, chlorine

Equation 1.1 represents a generalized chemical reaction between surface hydroxyl group and trimethylmethoxysilane [31].

$$Al\text{-}OH + CH_3\text{-}O\text{-}Si\text{-}(CH_3)_3 \rightarrow Al\text{-}O\text{-}Si(CH_3)_3 + HOCH_3 \tag{1.1}$$

Catalysts with 20 wt% cobalt promoted with 0.5 wt% rhenium were prepared by aqueous incipient wetness impregnation and modified in two ways, silane modification of γ-Al_2O_3 prior to cobalt impregnation and modification of catalyst after cobalt impregnation. Catalysts were characterized by hydrogen chemisorption, nitrogen adsorption, temperature programmed reduction (TPR), thermal gravimetric analysis (TGA), Fourier transform infra-red spectroscopy (FT-IR) and X-ray diffraction (XRD). Activity and selectivity of catalysts have been determined in a fixed bed reactor at 20 bar and 210 ^oC with H_2/CO ratio of 2.1.

Chapter 2

Fischer-Tropsch Synthesis

2.1 History

In the beginning of the 20th century, first experiments on the catalytic hydrogenation of carbon monoxide were carried out. A brief history of Fischer-Tropsch process is as follows [15].

- 1902 Sabatier and Senderens synthesized methane from a mixture of CO, CO_2 and H_2.
- 1922 Hans Fischer and Franz Tropsch proposed the Synthol Process to produce a mixture of aliphatic oxygenated compounds via reaction of CO and H_2.
- 1923 Important developments were made in FT process and Hans Fischer and Franz Tropsch published their first reports about hydrocarbon synthesis in 1926.
- 1934 FT process was licensed by Ruhrchemie and reached industrial maturity in 2 years.
- 1936 First large scale FT plant was operated in Braunkohle-Benzin.
- 1938 Germany reached a production capacity of 660 000 tons/year via FT process.
- 1955 Sasol plant in south Africa based upon both ARGE fixed bed and Kellog circulating bed catalyst was built.
- 1980's Fischer-Tropsch process again became the focus of research and development.
- 1993 Shell Bintulu plant with a production capacity of 12,500 barrels per day came into operation.
- 2006 Sasol Oryx 34,000 BPD plant inaugurated.

- 2011 Shell pearl GTL plant with the production capacity of 120,000 BPD started its production [32].

2.2 Technology

Fischer-Tropsch is an important process to convert syngas into liquid fuels. FT is categorised under indirect liquefaction as feed is first converted to syngas and then subsequently converted to liquid fuels. A block diagram of the process is shown in Figure 2.1.

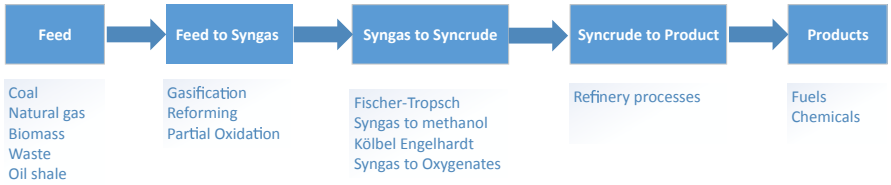

Figure 2.1: Simple block diagram of a Gas to Liquid process [33]

Fischer-Tropsch process can be divided into three main steps [33].

1. Feed gas conversion to syngas
2. Syngas to syncrude conversion
3. Syncrude to product conversion

Any kind of carbonaceous material like coal, natural gas or biomass can be used as a feed to produce syngas. Feed gas conversion is the most expensive and energy intensive step in the overall process [33]. Syngas can be produced via different kind of processes i.e partial oxidation, steam reforming, autothermal reforming or a combination. Choice of process depends upon the type of feed and the H_2:CO ratio required by the FT-process which is usually 2 as a rule of thumb [33]. Syngas cleaning is an inevitable step to get rid of all undesirable components and poisons for FT process. Sulfur is the most important poison for the FT catalyst. In addition, nitrogen containing compounds, bromides and oxygen can also cause poisoning [33]. CO_2 is also removed from the syngas during the cleaning step. Ratio of H_2:CO is also adjusted during this stage. Once the desired purity and ratio of syngas is achieved, it is fed to the FT reactor where it is converted to syncrude consisting of a range of paraffinic and olefinic products. In the final step the product is upgraded and refined to increase the yield of important commercial fractions like diesel and gasoline.

Due to the high exothermic nature of the Fischer-Tropsch synthesis, temperature control is an important challenge. Different kinds of reactors are used commercially for efficient management of heat namely [34].

- Fixed bed
- Fluidised bed

- Slurry bed

2.3 Reactions and Thermodynamics

Fischer-Tropsh process converts syngas catalytically into a range of hydrocarbons and oxygenated products through a series of polymerization reactions. The complex reaction chemistry can be simplified as follows [34, 35]

Main Reactions

$$\text{Methane} : CO + 3H_2 \rightarrow CH_4 + nH_2O \tag{2.1}$$

$$\text{Heavier Hydrocarbons} : nCO + 2nH_2 \rightarrow (-CH_2-)_n + nH_2O \tag{2.2}$$

Side Reactions

$$\text{Water Gas Shift} : CO + H_2O \rightarrow CO_2 + H_2 \tag{2.3}$$

$$\text{Alcohols} : nCO + 2nH_2 \rightarrow C_nH_{2n+2}O + (n-1)H_2O \tag{2.4}$$

$$\text{Boudard Reaction} : 2CO \rightarrow C + CO_2 \tag{2.5}$$

These reactions are quite simplified versions of the reality and the consumption of carbon monoxide and hydrogen depends upon extent of other reactions and secondary reactions. The extent of water gas shift (WGS) reaction can have a significant effect on the consumption. In case of cobalt catalyst, for which WGS reaction potential is almost negligible, the usage ratio is mainly governed by reaction 2.2 with a significant influence from reaction 2.1. The consumption ratio is typically between 2.06 and 2.16 depending on the extent of methane formation, olefin content in long chain hydrocarbon and the slight WGS reaction [35]. In case of iron catalyst which has a very high WGS potential, water gas shift reaction approaches equilibrium, the usage ratio depends upon the composition of the feed gas.

Under typical operating conditions, synthesis reactions are far from being in thermodynamic equilibrium [33] and highly exothermic; the formation of one mole of -CH2- is accompanied by a heat release of 145 kJ. Temperature has a significant affect on product selectivity and Fischer-Tropsch technologies are classified based on temperature in to low temperature FT (LT-FT $< 250\ ^o$ C) and high temperature FT (HT-FT $> 320\ ^o$ C). Increase in temperature leads to a shift in the carbon number distribution to lighter products [36]. Effect of pressure and synthesis gas depends upon the catalyst used and operating conditions.

2.4 Reaction Mechanism

Different mechanisms have been proposed for the FT reactions to explain the observed product distribution. Four most popular ones are carbide mechanism, enol mechanism, alkyl mechanism and CO-insertion mechanism. Common assumptions to all is that chain growth occurs by a step growth mechanism. The basic building blocks of the FT reactions are the 'CH_2' units, chemisorbed on the catalyst surface. The Fischer-Tropsch reaction is initiated by adsorption of carbon monoxide on the catalyst surface which further reacts

with hydrogen to produce a 'CH_2' unit. Chain growth propagates by subsequent addition of 'CH_2' units thus producing hydrocarbons ranging from methane to high molecular mass waxes. Chain termination either occurs by hydrogen addition yielding n-paraffain or by β-H-elimination resulting in olefin product. At steady state, the concentration of each 'C_nH_{2n}' species on the catalyst surfacce is constant. If the probability of chain growth is α then the probability of chain termination is (1-α). [35]

The probability of chain growth is defined by equation 2.6 in terms of the rate of polymerization (r_p) and the rate of termination (r_t) of the growing chains [36].

$$\alpha = \frac{r_p}{r_p + r_t} \tag{2.6}$$

Schulz-Flory equation (2.7) is used to calculate the carbon number distribution obtained during Fischer- Tropsch assuming that the chain growth is independent of the chain length [33].

$$x_n = (1 - \alpha).\alpha^{(n-1)} \tag{2.7}$$

where *n* is the carbon number, α is the chain growth probability and x_n is the molar fraction of each carbon number in the product. In order to calculate the α value from the molar fraction of each carbon number, equation (2.7) is often expressed in logarithmic form as in equation 2.8 [33].

$$log(x_n) = n.log(\alpha) + log[(1 - \alpha)/\alpha] \tag{2.8}$$

The carbon number distribution described by the Schulz-Flory equation is commonly referred to as the Anderson-Schulz-Flory (ASF) distribution [33]. The hydrocarbon spectrum calculated for α values ranging from zero to one is shown in Figure (2.2). All products except from "CH_4" and "C_{35}-C_{120}" go through a maxima as α increases. The FT products follow the ASF distribution except for the C_1 and C_2 [36]. From the Figure (2.2) it is evident that only methane and wax can be produced with high selectivity.

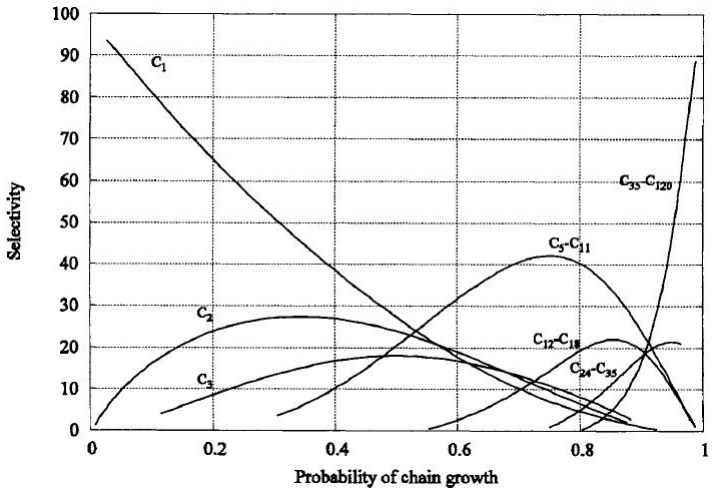

Figure 2.2: Product selectivity as a function of chain growth probability. Adapted from [35]

2.5 Catalysts

Good Fischer-Tropsch activity requires metals that allow dissociative CO adsorption and have H_2 adsorption behaviour [33]. Only the four group VIII metals, iron, cobalt, nickel and ruthenium possess adequately high activities for the hydrogenation of carbon monoxide, suitable for possible application in Fischer-Tropsch synthesis. Ruthenium has the highest activity but its low availability and high cost rules out its usage as industrial catalyst. Nickel is sufficiently active but it has two major drawbacks. It produces more methane due to its high hydrogenation potential. It also produces volatile nickel Carbonyls at the operating conditions of FT synthesis, resulting in continuous loss of metal. Therefore it is evident that only iron and cobalt based catalysts can be considered as practical FT catalysts. [37]

Only cobalt & iron are used industrially and an important difference between them is the potential for WGS reaction. Cobalt has less WGS activity thus making it suitable for syngas obtained from natural gas feed. Iron has very high WGS activity and produces more olefinic and oxygenates products. Iron is used for syngas derived from coal/biomass based feed. [37]

Chapter 3

Support Effects on Fischer-Tropsch Synthesis

In supported heterogeneous catalysis, active metal is dispersed on an high surface area support material. Ideally support should be a cheap material, having high surface area and inert characteristics. It should also posses sufficient thermal and mechanical stability at the reaction and regeneration conditions [38]. It is important to note that support can contribute to selectivity, activity and stability of the catalyst under operating conditions [39].

Most commonly used supports are oxide supports such as silica, alumina, zeolites and active carbons. Non-reducible oxides can be used as solid bases or acids. For example alumina has some acidic properties when calcined at lower temperatures while Cao, BaO and MgO have basic properties. Silica-alumina possesses strong acidic properties and has been used as a catalyst for hydrocarbon isomerisation [39].

3.1 Alumina

Aluminium oxide, alumina (Al_2O_3), is an interesting ceramic material which exists in many metastable structures (such as χ , κ, γ, η, ,δ, θ, α-Al_2O_3) which are called transition aluminas [40]. These polymorphs posses different structural and stability characteristics [38]. The thermodynamic stability of transition alumina follows the trend α-Al_2O_3 > θ-Al_2O_3 > γ-Al_2O_3 [41]. Among all the transitional aluminas, γ-alumina is the most commonly used support material [39].

Alumina finds extensive application in catalysis owing to its high thermal stability, moderate prices. Common applications of alumina as a support material in catalysis include [41].

- Hydrotreating of middle distillates via Co-Mo and Ni-Mo sulfides on alumia support.

- Vapor phase benzene hydrogenation via Pt/Al_2O_3 catalyst.
- Fischer-Tropsch synthesis via cobalt/alumina catalyst
- Production of vinyl chloride monomer by oxychlorination of ethylene to ethylene dichloride using copper chloride catalyst supported on alumina [42].

Alumina can have surface area varying from few m^2/g to 300 m^2/g, depending upon its texture and phase [38].

3.2 Effect of Support Variables on Fischer-Tropsch Synthesis

Most commonly used supports for cobalt based Fischer-Trposch catalysts are SiO_2, Al_2O_3, TiO_2 [16, 17]. Surface properties and texture of support have a significant effect on the reducibility and dispersion of cobalt catalysts [18, 19].

The type and structure of support have a significant effect on the particle size, dispersion, reducibility which thus affects the activity of the cobalt supported catalysts [1–4, 16, 20–27]. Type of the support and promoter used influences the C_{5+} selectivity [1, 21, 23, 25–27].

S. Storsæter et al. [43] investigated the effect of different support on the size, shape and reducibility of cobalt particles. They found that reducibility and Co^o particle size increases with increasing average pore diameter of support. C_{5+} selectivity is favored by large pores and thus large cobalt particle, particularly when external water is added. Borg et al. [44] also reported a positive correlation between the catalyst pore diamter and C_{5+} selectivity.

Zhang et al. reported that acidity of γ-Al_2O_3 has an effect on the reducibility of the cobalt. Higher Fischer-Tropsch activity and C_{5+} is shown by supports with low acidity [45].

Use of different transitional alumina as a support material affects the product distribution in the Fischer Tropsch synthesis. Selectivities for C_{5+} ranging in the order Co/α-Al_2O_3 > Co/δ-Al_2O_3 > Co/θ-Al_2O_3 > Co/γ-Al_2O_3 are obtained [28]. This effect of support material is not clearly understood and explained until now [46]. Probability of diffusional limitations leading to varied product distribution in these supports was ruled out by Rytter et al. [47]. Borg et al. suggested that the difference in chemical properties of α-Al_2O_3 and γ-Al_2O_3 can be the reason for difference in C_{5+} selectivities [30].

3.3 Surface Modified Supports for Cobalt Fischer-Tropsch Synthesis

Shi et al. [5] modified 10 wt% cobalt and 0.4 wt% ruthenium supported on SiO_2 catalyst with trimethylchlorosilane (TMCS). They observed a monotonic increase in C_5-C_{11} se-

lectivity with increasing surface coverage of modifier at 24 hrs on stream. The effect was attributed to the increased hydrophobicity of the catalyst.

In another research, Shi et al. [6] modified silica support with three different silanes, Methyltriethoxysilane (MTES), dimethyldiethoxysilane (DMDES), and chlorotrimethylsilane (TMCS). After modification, catalyst with 5 wt% cobalt loading was prepared by impregnation using ethanol as a solvent. An increase in CO conversion and and C_{5+} selectivity was observed with decrease in surface hydroxyl group concentrations at 24 h on stream.

Jia et al. [7] used vapor phase silylation for surface modification of SBA-15 using hexamethyldisilazane (HMDS). Cobalt catalysts with 20 wt% loading were prepared by impregnation using ethanol as a solvent. Samples were prepared by both pre-modification of support and post modification of catalyst. Modified catalysts showed a decrease in C_{5+} selectivity with post modified sample showing the highest decrease. An increase in CO conversion was reported for pre-modified samples. Pre-modified catalyst showed largest Co_3O_4 crystallite size and the highest reducibility. Weaker cobalt support interactions were believed to be the reason of larger cobalt size. Post modified catalyst exhibited poor catalytic performance.

Zhang et al. [48] used various organic solvents for silica support modification prior to cobalt impregnation. Pre-treatment with acetic acid resulted in an increase in CO conversion and C_{5+} Selectivity but a simultaneous decrease in turn over frequency (TOF) was also observed.

Ojeda et al. [8] also used hexamethyldisilazane (HMDS) for pre- and post-modification of 20 wt% Co/SiO_2 catalyst. They reported an increase in conversion and decrease in C_{5+} selectivity in post modified sample at 2300 min on stream.

J Zhang et al. [49] used organic solvents for treatment of γ-alumina support prior to active metal impregnation. Modified catalyst with 12 wt% cobalt loading supported on γ-Al_2O_3 were used for Fischer-Tropsch synthesis. In contrast to Zhang et al. [48], acetic acid modified supports showed smaller Co_3O_4 crystallite size, lowest CO conversion and C_{5+} conversion.

All these research groups compared catalytic performance of modified catalyst in terms of CO conversion and product selectivities at specific time on stream. It is important for a reliable comparison of Fischer-Tropsch catalyst to compare C_{5+} selectivities at same CO conversion level as C_{5+} selectivity is strongly dependent on the CO conversion [2, 43, 50]. In addition, activities of the catalysts are not reported at all, either in terms of site time yield (STY) or rate of reaction. STY is preferred when comparing catalyst with different metal loading as STY is independent of dispersion [2].

3.4 Surface Modification with Silanes

As established, supports have an effect on the performance of cobalt supported Fischer-Tropsch catalysts. Numerous efforts have been made to modify the supports in order to achieve better catalytic performance. Surface modification of supports is quite significant in this respect. Surface modification makes use of the presence of ample hydroxyl groups on the surface of the support. As a result of surface modification, support becomes hydrophobic and researchers have tried to make use of this effect. Borg et al. [29] investi-

gated the effect of water on the activity and selectivity of cobalt Fischer-Tropsch catalyst supported on γ-alumina with different pore sizes. The addition of water increased the C_{5+} selectivity with corresponding decrease in methane selectivity. Addition of water at a lower partial pressure ratio had a different effect on activity for supports having narrow and large pore sizes. It reduced for narrow pore sized catalyst while increased for large pore catalysts. Addition of water in higher partial pressure resulted in decreased rate of reaction and permanent deactivation.
For surface modification, organofunctional-silanes seem to be the best option. The main advantage of silanes as compared to other organic compounds lies in their ability to form bonds through several mechanisms. Silanes commonly used for surface modification have the general formula $R_n - Si - X_{4-n}$ (n=1-3) where R is an nonhydrolyzeable organic radical that imparts hydrophobicity and X is a hydrolyze-able ligand, capable of reacting with hyroxyl group and forming a stable bond. Most common X groups are methoxy, ethoxy and chlorine [11, 51].

Upon surface modification, silanes can form either monolayer or multilayer. If the silanes contains more than one active group i.e *'X'* then it has more tendency to form multilayer due to the polycondensation of $-Si - OH$ groups to form $-O - Si - O$ linkages. On the other hand if silane contains three organic groups and only one active group then silane is only capable of forming a monolayer [31].

3.5 Surface Structure of Supports

Surface structure of supports is very important in catalysis as catalysis is a surface phenomena. Both alumina and silica have hydroxyl groups on the surface which impart acidic character to the supports.

It is important to study the surface structure of silica and alumina support in order to understand the surface modification mechanism with silanes. Surface of both alumina and silica have hydroxyl groups but they cannot be treated in a similar way as they differ in dehydration behavior and reactivity.

3.5.1 Surface Structure of Alumina

Transitional aluminas have acidic properties which have significant importance in specific applications. Presence of significant concentration of hydroxyl groups on the surface of γ-Alumina gives rise to the acidic sites. These hydroxyl groups are formed either during the precursor decomposition or by subsequent interaction with atmospheric water. Figure 3.1 shows the formation of surface hydroxyl groups by the interaction of dehydrated γ-alumina surface with water.

The dehydrated surface is a Lewis acid whereas Brönsted acidic character is exhibited by surface $AlOH$ groups. If the surface is not fully hydrated, then it gives rise to a combination of Brönsted and Lewis acid character [39].

An interesting property of alumina which makes it an excellent support material is its ability to disperse the active phase that is attributed to the acid-basic character of alumina surface. The deposition or impregnation of active phase onto support is a true chemical reaction. Alumina, with its Lewis acidity, stable surface OH groups and the very high

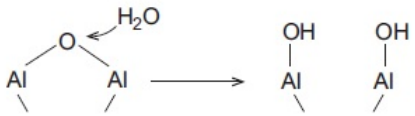

Figure 3.1: Formation of surface hydroxyl from the dehydrated γ-alumina. Adopted from [39].

polarity of the surface acid-base pairs, offers specific sites for anchoring anionic, cationic and metallic species. The acidity, attributed to surface hydroxyl groups, differs in different alumina polymorphs. It has been shown that high surface area γ-Al_2O_3 presents strong Lewis acid sites as compared to low surface area γ-Al_2O_3 [52]. This surface acidity provides a unique advantage of having acidic support which is effectively utilised in many catalytic systems.

Surface Modification of Alumina Supports

Recently various studies have been conducted to convert hydrophilic alumina into hydrophobic alumina. Chemical modification of the surface was carried out by using different modifiers like methyltrimethoxysilane (MTMS), tetraethylorthosilicate (TEOS), stearic acid and methyltrichlorosilane [9–11]. All these modifiers aim at complete substitution of the surface *-OH-* groups to induce hydrophobicity. Figure 3.2 shows the modification reaction of alumina with Trimethylmethoxysilane (TMMeS). During the reaction the methoxyl group combines with alumina through oxygen bonding while the organic group serves for inducing hydrophobicity. In the same fashion almost all of the surface hydrogens of *Al-OH* groups are replaced by *-Al-O-Si* bonds making the surface hydrophobic [31].

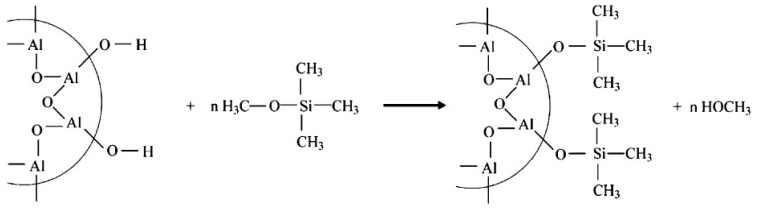

Figure 3.2: Surface modification reaction of alumina with Silane [31].

3.5.2 Surface Structure of Silica Support

Silica surface is reasonably acidic due to the presence of surface hydroxyl groups [39]. The structure of silica terminates at the surface with either a siloxane group ($\equiv Si-O-Si \equiv$) or as a silanol group ($\equiv SiOH$). Silanol groups can be divided into three classes (1) Isolated silanol (free silanols) (2) Vicinal Silanols (bridged silanols) (3) Germinal Silanols (bridged silanols) as shown in Figure 3.3 [51].

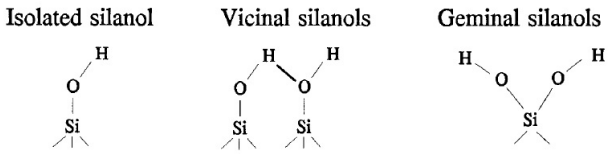

Figure 3.3: Silanol groups on silica surface. Adopted from [51].

In isolated silanols, silica has one bond to *-OH* and rest of the three bonds into the bulk structure. In vicinal silanol, the hydroxyl groups attached to two different silicon atoms are close enough to form hydrogen bonding. In geminal silanol, two hydorxyl groups are attached to a single silicon atom. The free silanols are sufficiently far enough to form a hydrogen bond. The concentration of bridged silanols increases with temperature exhibiting enhanced reactivity [51].

Surface of silica may be covered by vicinal as well as isolated hydroxyl groups. The reactivity of different silanol differs from each other and should be understood in detail to explain the surface modification. The reactivity of halogen silanes decreases in the order $(CH_3)SiI > (CH_3)SiBr > (CH_3)SiCl$. Alkoxy-silanes have increased reactivity with free silanols as compared to chloro-silanes. Reactivity of bridged and free silanols with chloro-silanes depends upon temperature and time of reaction. Chloro-silanes mostly react with free silanols with a smaller contribution from bridged silanols as well [51]. The extent of surface silanol group that reacts depends upon three factors [51].

- The ability of the silane to penetrate to inaccessible hydroxyl group. The smaller the size of reactant, the more surface groups modified.
- Bifunctional ability of the reactant leads to higher degree of modification.
- The steric hinderane of the chemisorbed species. The higher the steric hinderance, more it prevents the neighboring silanol groups to react.

Surface modification is carried out by reaction of these surface silanol groups with silanes.

Surface modification of Silica Supports

The modification can be carried out either in aqueous phase or hydrocarbon phase. Silanes undergo hydrolysis and condensation, in aqueous solvent, before deposition on the surface. Reaction mechanism is depicted in Figure 3.4. Alkoxy or halogen groups are hydrolyzed when they come in contact with water. The silanol groups thus formed, show hydrogen bonding towards neighboring silanol groups and also surface silanol groups. Formation of siloxane bond takes place with release of water. Subsequently polymerisation takes place at the surface of silica resulting in a three dimensional polymeric silane network [51].

Surface coating of silane consists of chemisorbed as well as physisorbed molecules. Physisorbed molecules condense slowly and a post-reaction curing step, consisting of heat treatment generally at 80-200 ^{o}C, is required for the chemical stabilization of the layer.

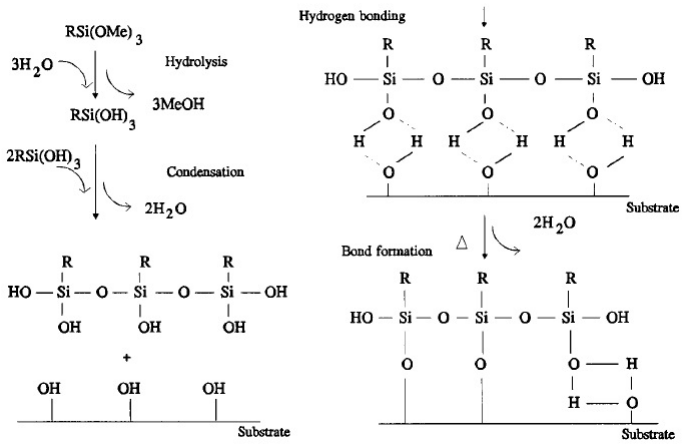

Figure 3.4: Mechanism of silane modification of silica in aqueous phase. Adopted from [51].

Hydrolysis rate of silanes is influenced by the functionality of the organic groups. With an increase in size of the organic group, the stability of the silanol also increase. As concentration of silane in modifier solution increases, amount of silane deposited increases up to a certain concentration and rate of deposition becomes slow above that concentration.

Hydrolysis is prevented if the modification with alkoxy-silanes or chloro-silanes is carried out in dry condition(dehydrated surface, dry organic solvent). Therefore silane should react with the surface by direct condensation of alkoxy- or chlorogroups with surface silanols. Blitz [53] reported that direct condensation does not occur in dry conditions. Presence of water is necessary for silane hydorlysis and subsequent reaction with the surface [51]. The reaction between silica surface and (methyl)chlorosilanes have been investigated by many researchers. Five possible reaction mechanism are suggested, which are believed to occur either simultaneously or consecutively [51].

3.6 Silanes Used for Surface Modification

Six different silanes varying in type of functional group, number of functional groups and size of organic group were selected in this research work. Chlorotrimethylsilane, methoxytrimethylsilane, dichlorodimethylsilane, chlorodimethyloctylsilane, methoxydimethyloctylsilane, trichloroctylsilane were used for surface modification. Table 3.1 summarizes the important properties of silanes used.

Chemical formulas and structures of the silanes used are shown in Figure 3.5.

Table 3.1: Silanes used for surface modification

Silane	Alternate Name[a]	Abbreviation[b]	Mol. Weight	Boiling Point [^{o}C]
Methoxytrimethylsilane	Trimethylmethoxysilane	TMMeS	104.22	57-58
Methoxydimethyloctylsilane	–	DMMeOS	202.41	221 - 223
Chlorotrimethylsilane	Trimethylchlorosilane	TMCS	108.64	57
Chlorodimethyloctylsilane	Dimethyloctylchlorosilane	DMOCS	206.83	222 - 225
Dichlorodimethylsilane	Dimethyldichlorosilane	DMDCS	129.06	70
Trichloroctylsilane	Octyltrichlorosilane	OTCS	247.67	233

(a) Reported in MSDS
(b) Abbreviation key, T = Tri, M= Methyl-, Me=Methoxy-, C=Chlro-, O=Octyl-, S=Silane

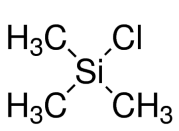

(a) Chlorotrimethylsilane
$((CH_3)_3SiCl)$

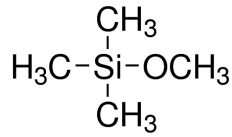

(b) Methoxytrimethylsilane
$(CH_3OSi(CH_3)_3)$

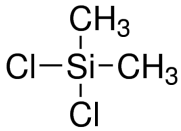

(c) Dichlorodimethylsilane
$((CH_3)_2SiCl_2)$

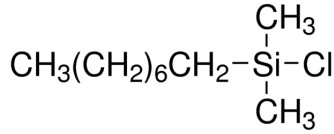

(d) Chlorodimethyloctylsilane
$(CH_3(CH_2)_7Si(CH_3)_2Cl)$

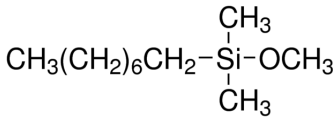

(e) Methoxydimethyloctylsilane
$(CH_3(CH_2)_7Si(CH_3)_2OCH_3)$

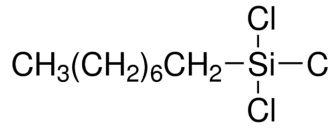

(f) Trichloroctylsilane
$(CH_3(CH_2)_7SiCl_3)$

Figure 3.5: Silanes used for surface modification of γ-Alumina

Depending upon the type of active/functional group, silanes can be classified into two classes: *methoxy-silanes* and *chloro-silanes*. Out of six silanes used, two were classified as *methoxy-silanes* and both of them contain same number of functional groups i.e 1, but they differ in the length of the organic group. Methoxytrimethylsilane contains three *-(methyl)* groups while methoxydimethyloctylsilane comprises one *-(octyl)* and two *-(methyl)* groups. Table 3.2 summaries the important structural characteristics of silanes.

Chloro-silanes differ in two respects, number of active groups and length of organic groups. Number of active groups varies from one to three. Both chlorotrimethylsilane

and chlorodimethyloctylsilane contain only one active group but differ in terms of organic group. Only dichlorodimethylsilane contains two functional groups with *-(methyl)* as the organic group. Trioctylsilane contains highest number of functional groups i.e 3 as well as the bulkiest *-(octyl)* side group.

Table 3.2: Chemical structure analysis of the silanes used for surface modification

Silane	Active group	No of active groups	Organic group
Methoxytrimethylsilane	$-OCH_3$	1	*-Methyl*
Methoxydimethyloctylsilane	$-OCH_3$	1	*-Octyl*
Chlorotrimethylsilane	*-Cl*	1	*-Methyl*
Chlorodimethyloctylsilane	*-Cl*	1	*-Octyl*
Dichlorodimethylsilane	*-Cl*	2	*-Methyl*
Trichloroctylsilane	*-Cl*	3	*-Octyl*

Ability of the silane to form mono- or multilayer on the surface depends upon the number of active groups. The presence of one functional group permits only monolayer formation [31]. Four of the silanes used contain only one functional group whereas dichlorodimethylsilane and trichloroctylsilane contained two and three chlorine functional groups respectively.

Length of the bulky group dictates the maximum extent of surface modification possible. Eakins et el. reported a maximum of 60% surface modification of silica with trimethylsilane [54]. The extent of surface modification decreases with increase in size and steric hinderance of bulky groups. Two of the silanes used contained *-(trimethyl)* organic group, one contained *-(dimethyl)* organic group and two contained *-(dimethyloctylmethyl)* group.

Chapter 4

Theory

4.1 Catalyst Preparation

Heterogeneous catalysts can be broadly divided into two classes: Bulk (unsupported) and supported catalysts. Figure 4.1 shows the main steps involved in the two routes

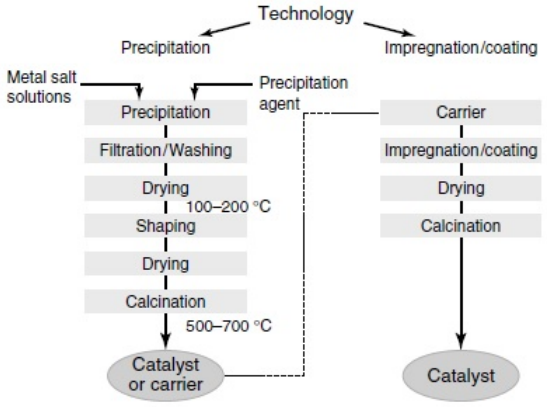

Figure 4.1: Preparation route of heterogeneous catalyst. Adapted from [38]

Traditionally heterogeneous catalysts are prepared by impregnation methods consisting of immersing the solid in a solution of metal salt and inducing deposition. The support is dried to remove the extra liquid and in the final step it is calcined at higher temperature to get the final catalyst.

Impregnation can be sub classified into two classes depending upon the relationship between support pore volume (V_p) and liquid volume (V_{imp}) : (1) Wet impregnation (2) Dry/Incipient wetness impregnation. Impregnation is called wet impregnation when liquid

volume is greater than support pore volume $V_{imp} > V_p$ whereas in incipient wetness impregnation the volume of the impregnating solution is equal to the pore volume of the support bodies $V_{imp} \approx V_p$. [55]. This method offers several advantages- no risk of loss of precious precursor and no production of waste water. Impregnation method is mostly employed for impregnation of precious metals onto the support [38].

After impregnation, the sample is dried to evaporate the acqueous phase and finally calcined. Calcination is performed to thermally decompose nonoxide precursor, oxidise the support and surface species and remove unwanted ligands [55].

4.2 Catalyst Characterisation

Catalysts were characterized by hydrogen chemisorption, nitrogen adsorption, temperature programmed reduction (TPR), thermal gravimetric analysis (TGA), Fourier transform infra-red spectroscopy (FT-IR) and X-ray diffraction (XRD). Activity and selectivity of catalysts have been determined in a fixed bed reactor at 20 bar and 210 ^{o}C.

4.2.1 Hydrogen Chemisorption

Chemisorption is one of the most important catalyst characterisation techniques to determine metal dispersion defined as

$$D = \frac{\text{Metal atoms deposited on the surface}}{\text{Total number of metal atoms}} \tag{4.1}$$

Dispersion can be calculated by knowing the amount of gas adsorbed at monolayer coverage given that the adsorption stoichiometry is known. Adsorption stoichiometry refers to the number of surface metal atoms associated with the adsorption of each adsorbed gas molecule.

Different gases can be used as adsorbate but H_2, CO and O_2 are most commonly used [38]. An ideal adsorbate gas should adsorb irreversibly and should have minimum or no adsorption on support material. Choice of gas depends upon nature of the metal and the operating conditions. Adsorption isotherms are obtained by successively increasing the pressure and determining the amount of gas adsorbed while keeping the temperature constant. To calculate the amount of gas chemisorbed at monolayer i.e v_m the isotherm is extrapolated back to zero pressure as shown in figure 4.2. [38]. The metal surface area and dispersion are calculated by equations 4.2 and 4.3 [38]

$$A = \frac{v_m}{22414} N_A \frac{n}{m} a_m \frac{100}{wt} \tag{4.2}$$

$$D = \frac{v_m n}{22414 m} / \frac{wt}{100 M} \tag{4.3}$$

where v_m is expressed in cm^3 (STP), N_A is the Avogadro's number (6,022 * 10^{23} mol^{-1}), n the chemisorption stoichiometry, m the mass of the sample (g), a_m the surface area (m^2) occupied by a metal atom, wt (%) the metal loading and M is the atomic mass of the metal.

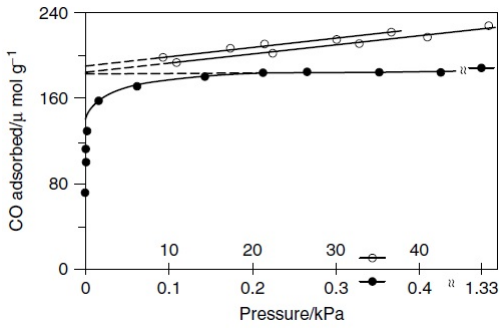

Figure 4.2: Isotherms for the adsorption of CO on EUROPT-1 Pt/SiO_2 catalyst at room temperature from different laboratories for a pressure range 0 - 1.33 kPa (solid circles) and 10 - 50 kPa (open circles) [38]

Hydrogen generally adsorbs dissociatively according to the equation 4.4.[38]

$$H_2 + 2M_S \rightarrow 2M_S - H \tag{4.4}$$

where M_s represents a surface metal atom. The adsorption of hydrogen on cobalt is also dissociative i.e n = 2, one hydrogen molecules occupies two cobalt sites.

4.2.2 Nitrogen Adsorption

Nitrogen adsorption is used to calculate the surface area of supports and catalysts. The method is based on the physisorption of N_2 on a certain amount of material. The gas uptake is measured at a constant low temp (-193 ^{o}C) as a function of N_2 pressure and is usually well described by Brunauer-Emmett-Teller (BET) isotherm [56]. BET equation(4.5) is a further development of the Langmuir isotherm to describe the multilayer adsorption and in addition to Langmuir isotherm assumptions it is based on the following assumptions [56].

- Heat of adsorption for the first layer is constant.
- Heat of adsorption for the second and the subsequent layers is equal to the latent heat of evaporation.
- A dynamic equilibrium exists between each layer and gas phase.

$$\frac{p}{V(p_0 - p)} = \frac{1}{V_m c} + \frac{c-1}{V_m c} . \frac{p}{p_0} \tag{4.5}$$

Where V is the volume of the adsorbed gas, p is the pressure of the gas, p_0 is the saturated vapour pressure of the liquid at the operating temperature and V_m is the volume equivalent to an adorbed monolayer and c is a constant [57].

BET surface area calculation involves two stages. Firstly physisorption isotherm is transformed to a BET plot and BET monolayer capacity is derived from it. Secondly, specific surface area is calculated which requires a knowledge of the molecular area [38]. Plotting of $\frac{p}{V(p_0-p)}$ vs $\frac{p}{p_0}$ gives a linear BET plot and the constant "c" and monolayer

coverage can be easily calculated from the slope and the intercept of the straight line respectively. The number of molecules is calculated from the monolayer coverage and knowing the area occupied by one nitrogen molecule $\sigma_N = 0.162nm^2$ [38], the total BET surface area per gram of material can be calculated. Although BET method is widely used for surface area measurement, it has some limitations as well. It is based on oversimplified model of physiosorption, so as a consequence, this method is used only in an empirical manner. Also the assumption about the constant packing of N_2 molecules does not hold in each case due to adsorbate structure [38].

4.2.3 Temperature Programmed Reduction (TPR)

In a TPR experiment, the sample is loaded inside a fixed bed reactor, temperature is ramped at a specific rate, with a specific flow rate of reducing gas i.e hydrogen. Gas compositions are analyzed by using thermal conductivity detector (TCD) or mass spectrometer (MS). The consumption of hydrogen is recorded against the temperature and plotted as TPR spectrum.

TPR results are typically discussed in a qualitative manner mainly due to the complexity of the reduction processes [38]. The most useful information obtained from the TPR analysis is the temperature required for the complete reduction of the catalyst. It also reveals the information that either the reduction is single step or multi step. Effect of promoter, support of metal loading on reduction temperature can be also be studied.

4.2.4 X-ray Diffraction

X-ray diffraction is one of the most frequently used characterization techniques for identification of the crystalline phases inside catalysts and estimation of the crystallite size. X-rays, on the crystalline sample, are elastically scattered by atoms in the periodic lattice. Scattered monochromatic X-rays that are in phase undergo constructive interference, as shown in Figure 4.3 [56].

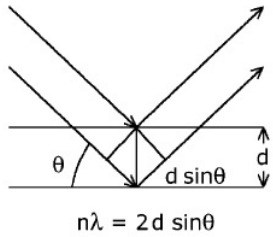

Figure 4.3: Constructive interference of scattered X-rays by crystal lattice governed by Bragg's Law adopted from [56]

Constructive interference occurs when Bragg's Law is satisfied [56]

$$n\lambda = 2dSin\theta \tag{4.6}$$

where *n* is an integer called order of reflection, λ is the wavelength of the X-rays, *d* is the lattice spacing, θ is the angle between the incident X-rays and the normal to the reflecting lattice plane.

The diffraction peaks are unique for each crystalline phase, possessing a long range order, and width of the peak carries information about the dimensions of the reflecting plane. Scherrer formula relates the crystallite size to the peak width. [58]

$$d_v = \frac{K\lambda}{\beta Cos\theta} \tag{4.7}$$

where d_v is the volume-weighted crystallite diameter, λ is the wavelength of X-rays, β is the line broadening of a particular peak due to the crystallite size, θ is the angle of the diffraction peak and *K* is a constant. Assuming uniform and spherical crystallites, a geometrical factor of 4/3 is applied to crystallite thickness to get the average spherical Co_3O_4 particle size as shown in equation 4.8 [59]. The diameter of the metallic cobalt is calculated by multiplying average spherical particle size by a factor of 0.8 as shown by equation 4.9. [60].

$$d(Co_3O_4) = \frac{4}{3}.d_v(Co_3O_4) \tag{4.8}$$

$$d(Co) = 0.8.d(Co_3O_4) \tag{4.9}$$

where $d(Co_3O_4)$ and $d(Co)$ are the particle sizes of cobalt oxide and metallic cobalt respectively.

4.2.5 Fourier Transform Infra-red Spectroscopy (FT-IR)

Infrared spectroscopy is a vibrational spectroscopy technique, which has found wide spread applications in catalysis. Sample is subjected to Infrared waves, molecules vibrate upon absorption of specific wavelengths depending upon chemical structure. An IR spectrum is obtained by plotting the intensity of infrared (%transmittance or % absorbance) against the wavenumber. Interpretation of the infrared spectrum can help from simple qualitative analysis to in depth quantitative analysis revealing information about the molecules present and their concentration. [61, 62]

Infrared can be divided into three regions depending upon the wave number as shown in Table 4.1. Infrared spectroscopy is mostly performed in mid-IR region

Table 4.1: Infrared Regions

Infrared	**Wavelength** (cm^{-1})
Near IR	14,000-4000
Mid IR	4000-400
Far IR	400-4

Attenuated total reflection (ATR) is the FT-IR sampling technique, that focuses on obtaining spectral information from reflection properties. ATR is a contact sample technique that measures the changes that occurred in a totally reflected infrared beam as it comes into contact with the sample. A good contact between sample and crystal surface is important to ensure good quality of results. Advantage of ATR is that it requires no sample preparation, quick and non-destructive [62].

4.2.6 Thermal Gravimetric Analysis

TGA is used to measure the microscopic weight changes either as function of increasing temperature or isothermally as function of time in a gas atmosphere like helium, air, carbon monoxide or in vacuum [63].

A small amount of catalyst is loaded into a quartz pan suspended in a microbalance. A controlled gas flow and temperature ramp is initiated and a profile of weight change versus temperature is recorded. TGA units are frequently coupled with mass spectrometer to analyse the off gasses as the function of temperature. The weight temperature curves are used to characterize materials through analysis of the decomposition patterns, establishing procedures for regenerating the catalyst and studies of degradation patterns.

4.2.7 Activity and Selectivity Measurement

Activity and selectivity of the catalysts are determined in fixed bed reactor with Fischer-Tropsch synthesis carried out at 20 bar and 210 ^{o}C with H_2/CO = 2.1. Detailed process flow diagram of FT rig is given in Appendix F. Gas chromatography analysis is used to calculate gas conversion and selectivity. Activity is reported in terms of site time yield (s^{-1}).

Site-Time Yield

Site Time Yield (STY) is defined as the number of molecules of a specific product produced per catalytic site and per unit time [64]. STY is calulated by using Equation 4.10.

$$STY = \frac{r_{CO}.M}{w_m.D} \tag{4.10}$$

Where M is the molecular weight of the active metal, cobalt in this case, w_m is the weight fraction of active metal, and D is the dispersion.

STY is quite similar to turn over frequency but not identical. Turn over frequency is defined as *the number of revolution of catalytic cycles per second* [64]. In Fischer-Tropsch synthesis, it is quite difficult to measure the completion of catalytic cycle because of the polymerization reactions. Therefore Site Time Yield is more convenient for reporting of activity of catalyst having C+ as the specified product. Reporting activity in terms of TOF or STY offers several advantages. It is possible to compare the results of STY/TOF produced in different laboratories provided that the conditions and methods of measurement of rate, method of counting active sites are fully described. It can also be a measure of the life time of the catalyst by showing how many cycles a catalyst lasts before dying [64].

4.2.8 Gas Chromatography

Gas chromatography is an analytical technique used for separation and analysis of volatile compounds. Components of the sample under analysis are partitioned between two different phases, a stationary phase with a large surface area and a mobile gas phase ,as the sample is carried along by the mobile phase over the stationary phase bed in a separation column. The extent of partition of the components between the two phases depends upon respective solubility in each phase. Components having greater solubility in stationary phase take longer to emerge from the stationary phase bed as compared to those with less solubility. The partition equilibrium between the solute and the stationary phase is controlled by distribution constant, K_c defined as [65, 66]

$$K_c = \frac{A_S}{A_M} \tag{4.11}$$

where A_S is the concentration of the component A is stationary phase and A_M is the concentration in the mobile phase. In gas chromatography mobile phase is an inert gas usually helium, hydrogen or nitrogen and stationary phase is high molecular weight liquid deposited either on the walls of a long capillary tube or on the surface of finely divided particles. A modern gas chromatograph consists of (1) Carrier Gas (2) Flow Controller (3) Sample inlet / injector (4) Column (5) Controlled temperature zones (6) Detectors (7) Data system. The inert carrier gas flows through the injection port, the column and the detector. Carrier gas flow rate is carefully controlled to minimize detector noise and ensure reproducible retention times. The sample is injected into heated injection port, where it is vaporised (if necessary) prior to introduction to separation column. The sample partitions into individual components in the column depending upon relative affinity for the liquid phase and relative vapor pressures. Upon exiting the column, sample and carrier gas pass through a detector which is insensitive to carrier gas, measures the quantity of the sample and generates an electrical signal. Most commonly used detectors are flame ionisation detector (FID), thermal conductivity detector (TCD) and electron capture detector (ECD). Data handling system generates a chromatograph based upon these signal [65, 66].

Chapter 5

Experimental

5.1 Catalyst Preparation

A Catalyst with 20 wt% cobalt and 0.5 wt% rhenium on alumina (Co/γ-Al_2O_3) was selected as reference catalyst for the study. Catalyst was prepared by one step incipient wetness impregnation of γ-Al_2O_3 support (53-90 μm) with aqueous solutions of cobalt nitratehexahydrate $Co(NO_3)_2.6H_2O$ and perrhenic acid $HReO_4$. Catalyst was sieved to the size range of 53-90 μm in order to ensure elimination of diffusion limitations during the Fischer Tropsch reactions [50, 67].

The incipient wetness point of the γ-Al_2O_3 support was determined by drop wise addition of deionized water. Values of incipient wetness points are given in Appendix C. After calculation of water required, calculations were performed for the amount of precursor salts required, keeping in mind that the salts were hydrated. Precursor solution was prepared and stirred until it was homogenized. It was then added gently to the support and dried in ventilated oven at 120 ^{o}C for 2 hours. It was stirred every quarter in the first hour and every half an hour in the second hour.

The dried sample was calcined in a fixed bed quartz reactor under 0.7L/(g.h) air flow at 300 ^{o}C with a temperature ramp rate of 2 ^{o}C/min for 16 hrs.

Calculations for the preparation of the reference catalyst can be found in Appendix B.

5.2 Surface Modification

Various samples were prepared by treating either support or reference catalyst with different silanes. Same concentration of modifier solution i.e 1% v/v silane/n-hexane was used for preparation of all samples. Modified samples were denoted as Co/(γ-Al_2O_3)$_{x.n}$. Where "x" denotes method of preparation i.e Pr = pre-modified and Po = Post-modified and "n" denotes the silane. n=1 is for methoxy-silanes for both pre- and post-modified samples. Details are shown in Table 5.1.

Table 5.1

Catalyst	Silane used	Modification Method[a]
Co/(γ-Al_2O_3)$_{Pr1}$	Methoxytrimethylsilane	Pre-modification
Co/(γ-Al_2O_3)$_{Pr2}$	Chlorotrimethylsilane	Pre-modification
Co/(γ-Al_2O_3)$_{Pr3}$	Dichlorodimethylsilane	Pre-modification
Co/(γ-Al_2O_3)$_{Pr4}$	Chlorodimethyloctylsilane	Pre-modification
Co/(γ-Al_2O_3)$_{Po1}$	Methoxydimethyloctylsilane	Post modification
Co/(γ-Al_2O_3)$_{Po2}$	Trichloroctylsilane	Post modification

5.2.1 Modification Procedure

A modified version of the method adopted by Weiwei et al. aiming at complete substitution of the surface hydrogen groups to yield superhydrophobic alumina aerogel was used. [10].

Surface modification was carried out by immersing 5g of sample in 100 ml of 1% v/v solution of silane/n-hexane, contained in a three neck round bottom flask, placed in an oil bath preheated to 50 ^{o}C. All reaction products were kept at 50 ^{o}C while being magnetically stirred for 24 hours. A local thermometer was used to monitor the actual temperature of the reaction mixture. Cooling water at an appropriate flowrate was used to condense any evaporating n-hexane in order to keep concentration of the modification mixture constant. After 24 hours of operation, reaction mixture was cooled down, modified sample was separated from the silane/n-hexane solution by centrifugation and subsequent washing with n-hexane three times. Experimental setup is graphically depicted in Figure 5.1. Calculations for the preparation of the modification mixtures can be found in Appendix D.

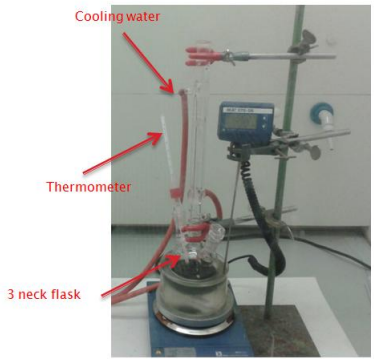

Figure 5.1: Experimental setup for surface modification

Modification methods can be divided into two classes with respect to execution order of modification and cobalt impregnation.

- **Pre-modification**: Surface modification of γ-Al_2O_3 support and subsequent incipient wetness impregnation of cobalt and rhenium.

- **Post modification**: Incipient wetness impregnation of cobalt and rhenium on γ-Al_2O_3 support and subsequent surface modification.

Pre-treatment of γ-alumina was carried with all the silanes and then subsequent impregnation of cobalt. Only methoxydimethyloctylsilane and trichloroctylsilane were prepared by post modification as they yielded completely hydrophobic supports prohibiting incipient impregnation with water.

5.2.2 Pre-modification of γ-Al_2O_3 Support

Figure 5.2 shows a block diagram of pre-modification procedure. γ-Al_2O_3 support was surface modified by procedure mentioned in section 5.2 and subsequently followed by active metal deposition by incipient impregnation method as mentioned in section 5.1. Catalyst prepared by methoxytrimethylsilane, chlorotrimethylsilane, dimethyldiclorosilane and chlorodimethyloctylsilane modified supports were prepared by this method and denoted as Co/(γ-Al_2O_3)$_{Pr1}$, Co/(γ-Al_2O_3)$_{Pr2}$, Co/(γ-Al_2O_3)$_{Pr3}$, Co/(γ-Al_2O_3)$_{Pr4}$.

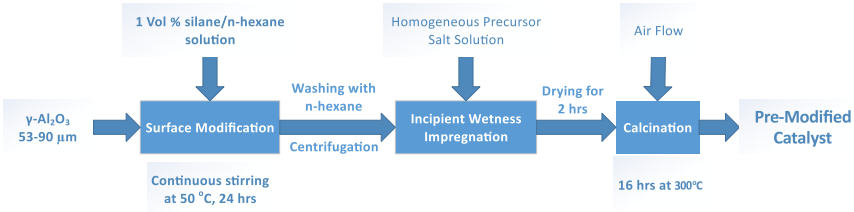

Figure 5.2: Block diagram of pre-modification method for preparation of surface modified catalyst

5.2.3 Post modification of Reference Catalyst

Figure 5.3 shows a block diagram of post modification procedure. Catalyst with 20 wt% Cobalt and 0.5 wt% Rhenium loading was prepared by the procedure mentioned in section 5.1 and subsequently surface modified by procedure mentioned in section 5.2.

Reference catalyst was surface modified with methoxydimethyloctylsilane and trichlorooctylsilane and denoted as Co/(γ-Al_2O_3)$_{Po1}$ and Co/(γ-Al_2O_3)$_{Po2}$.

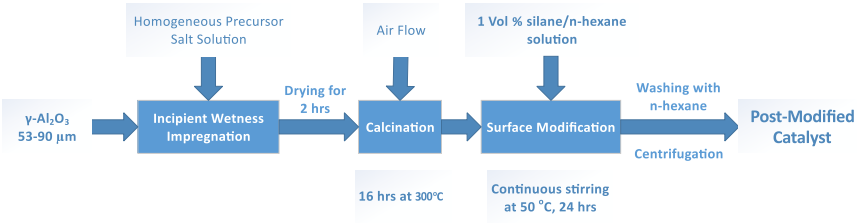

Figure 5.3: Block diagram of post modification method for preparation of surface modified catalyst

5.3 Catalyst Characterisation

Reference catalyst and modified samples were characterized by hydrogen chemisorption, nitorgen adsorption, temperature programmed reduction, X-ray diffraction, Fourier transform infra-red spectroscopy. Activity and selectivity of catalysts were determined in fixed bed reactor at 20 bar and 210 ^{o}C with H_2/CO ratio of 2.1.

5.3.1 Hydrogen Chemisorption

Dispersion for different samples was measured by using a Micromeritics ASAP-2010N unit. The catalyst was loaded (around 100 mg in each case), between two layers of quartz wool, in U-shaped quartz reactor. A thermocouple was used to measure the temperature of the sample under consideration. Thermocouple was located outside the reactor at the same height as the sample. The reactor was placed inside an electric furnace. The samples were first evacuated for about two hours and manual leak test was performed to ensure minimum pressure drop change of 50 μmHg/min.

After successful leak test, the automatic analysis sequence was started. The sample was first evacuated at 40 ^{o}C for one hour and leak test performed again. The temperature was increased to 350 ^{o}C at the rate of 1 ^{o}C/min in continuous flow of hydrogen for in-situ reduction of catalyst. After reduction, the samples were evacuated for 1 hour at 330 ^{o}C, evacuated for 30 minutes at 100 ^{o}C and finally cooled down to 40 ^{o}C. The analysis was performed at 40 ^{o}C. The analysis sequence is summarized in Table 5.2.

For the purpose of cobalt dispersion measurement, it was assumed that rhenium and support do not adsorb any hydrogen. An adsorption isotherm was constructed by measuring the amount of hydrogen adsorbed at 40 ^{o}C at 11 different values of pressure ranging from 15-500 mmHg. After the adsorption isotherm is obtained, dispersion is calculated by the procedure mentioned in section 4.2.1.

Table 5.2: Chemisorption Analysis Conditions and Sequences

Task Number	Analysis Step	Temp [^{o}C]	Time [min]
1	Evacuation	40	60
2	Leak Test	40	1
3	Hydrogen Flow	350	600
4	Evacuation	330	60
5	Evacuation	100	30
6	Leak test	100	1
7	Analysis	40	255

5.3.2 Nitrogen Adsorption

BET surface area was measured by using Micromeritics TriStar 3000 instrument by adsorption of nitrogen at liquid nitrogen temperature i.e -196 ^{o}C. The samples were degassed

at 200 ^{o}C overnight prior to measurement. Amount of sample used in each case was around 100 mg.

Physisorption isotherm was obtained and procedure mentioned in section 4.2.2 was used to calculate the BET surface. Based on the Barrett-Joyner-Halenda (BJH) model [68], the pore-size distribution and the pore volume of all the catalysts samples were determined.

5.3.3 Temperature Programmed Reduction (TPR)

TPR profiles of catalysts were recorded using a Altamira Benchcat Hybrid-1000HP unit. Samples (approximately 100 mg) were charged in a U-shaped quartz reactor (in between two quartz wool layer). The reactor was mounted in an electric furnace. Temperature of the catalyst bed was measured by a thermocouple inserted in the sample. The TPR was performed using a 10% H_2/Ar gas mixture at a flow rate of 50 cm^3/min. The catalyst samples were heated from ambient temperature to 800 ^{o}C at a rate of 10 ^{o}C/min. A thermal conductivity detector was used to measure the hydrogen consumption as a function of temperature.

5.3.4 X-ray Diffraction

The XRD apparatus Bruker D8 Advance DaVinci X-Ray Diffractometer - D8 DaVinci 1 with CuKα radiation was used for obtaining the XRD profiles spectra. The catalysts were prepared in the sample holders, and the 2θ angles chosen ranged from 15 to 75 ^{o} with 15 seconds steps in 30 minutes.

Raw XRD data was converted using the program PowDLL [69]. Pawley [70] fit of the obtained data sets was applied with fityk [71] for acquisition of FWHM. A K value of 1 and instrumental broadening 0.024^{o} 2 θ was used in Scherrer equation for calculation of crystallite size of Co_3O_4.

5.3.5 Thermal Gravimetric Analysis

Thermal gravemetric analysis were performed using Netzsch STA 4496. The samples, approximately 10 mg, were heated from room temperature to 800 ^{o}C at a rate of 10 ^{o}C/min with an air flow of 75 ml/min. Mass spectrometer was coupled with TGA and analysis was performed for chlorine, methane, silicon, water and carbon dioxide.

5.3.6 Fourier transform infrared Spectroscopy

The samples were investigated in ATR FTIR using a Nicolet IS50 FTIR KBr Gold Spectrometer using ATR diamond crystal. A 60 psi pressure tower was used to increase contact between crystal and sample. Absorbance spectra were acquired using a resolution of 4 cm^{-1} over a wave number from 400-4000 cm^{-1}. An empty cell was used as background at room temperature.

5.3.7 Activity and Selectivity Measurement

Activity and selectivity of the catalysts were determined in fixed bed reactor with Fischer-Tropsch synthesis carried out at 20 bar and 210 ^{o}C with H_2/CO = 2.1. Detailed process flow diagram of FT rig is given in Appendix F. Gas chromatography analysis is used to calculate gas conversion and selectivity.

Activity is reported in terms of site-time yield (s^{-1}). The selectivity of C_{5+} hydrocarbons was calculated by subtracting the amount of C_1C_4 hydrocarbons and CO_2 in the product gas mixture from the total mass balance. When C_{5+} selectivity is given as a single value, it refers to the value calculated at 50$\pm$1 % CO conversion.

Fischer Tropsch Synthesis Experiment

Fischer Tropsch synthesis was carried out in fixed bed reactors made of stainless steel and having an inner diameter of 10mm. All catalyst samples ca 1g, were diluted with 20g of silicon carbide in order to ensure isothermal conditions inside the reactor. The catalyst samples were loaded between quartz wool inside the reactor in order to keep the samples in place. After mounting the reactors on the experimental setup, the reactors were surrounded by aluminium blocks to ensure uniform heat distribution and minimize temperature gradient inside the reactor. An electric furnace was used for heating.

Prior to the start of experiments, the reactors were leak tested by pressurising with helium up to 20 bars. The catalysts were reduced insitu at 350 ^{o}C with hydrogen flowing at 250 ml/min with temperature ramped at the rate of 1 ^{o}C/min for 10 hrs. After reduction, the samples were cooled down to 170 ^{o}C and hydrogen was replaced with helium. The pressure was increased to 20 bars and the helium was replaced with syngas at a flowrate of 250ml/min. Syngas comprised 31.4 mole % CO and 65.6 mole % hydrogen with helium as internal standard. To avoid runaway and catalyst deactivation, the catalysts were heated to the operating temperature of 210 ^{o}C in three stages. First from 170 ^{o}C to 200 ^{o}C, then to 208 ^{o}C and finally to 210 ^{o}C with ramp rates of 20 ^{o}C/min, 5 ^{o}C/min and manual adjustment respectively. Heavier products like hydrocarbon wax and liquid products were removed in the hot trap (85-95 ^{o}C) while lighter components were removed in cold trap (25 ^{o}C). Compositions of both feed and product gas were measured using a gas chromatograph.

Chapter 6

Results and Discussion

Alumina support was modified with silanes by procedure mentioned in section 5.2.1 to yield six surface modified alumina samples. Details of the samples are given in Table 6.1

Table 6.1: Surface modified γ-Al_2O_3 samples

Sample	**Surface Modifier**	
	Silane	Abbreviation
(γ-Al_2O_3)	Un-modified	–
$(\gamma\text{-}Al_2O_3)_{Pr1}$	Methoxytrimethylsilane	TMMeS
$(\gamma\text{-}Al_2O_3)_{Pr2}$	Chlorotrimethylsilane	TMCS
$(\gamma\text{-}Al_2O_3)_{Pr3}$	Dichlorodimethylsilane	DMDCS
$(\gamma\text{-}Al_2O_3)_{Pr4}$	Chlorodimethyloctylsilane	DMOCS
$(\gamma\text{-}Al_2O_3)_{Po1}$	Methoxydimethyloctylsilane	DMMeOS
$(\gamma\text{-}Al_2O_3)_{Po2}$	Trichloroctylsilane	OTCS

6.1 Surface Modification of γ-Al_2O_3 Support

Silane modification aims at rendering hydrophobic surface by forming alkylsilyl layer on the surface. Surface modification of supports was investigated by analytical hydrophobic test and FT-IR spectra.

Hydrophobic nature of surface modified supports was checked analytically by absorption of water. Methoxydimethyloctylsilane ($(\gamma\text{-}Al_2O_3)_{Po1}$) and trichloroctylsilane ($(\gamma\text{-}Al_2O_3)_{Po2}$) modified supports displayed complete hydrophobic characteristics. Rest of the samples absorbed water but displayed reluctance in absorption of water indicating partial hydrophobic characteristics.

FT-IR analysis was used to characterize surface of modified supports. Figures 6.1 and 6.2 show the FT-IR spectra of modified supports.

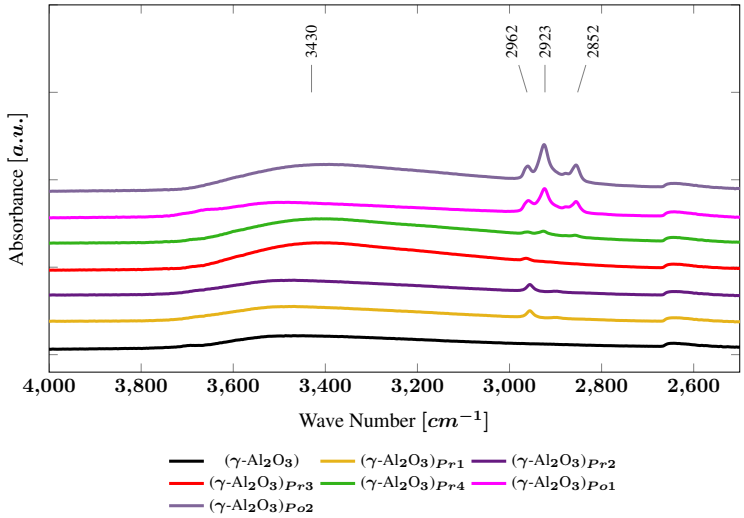

Figure 6.1: FT-IR spectra (4000-2500 cm^{-1}) of surface modified supports.

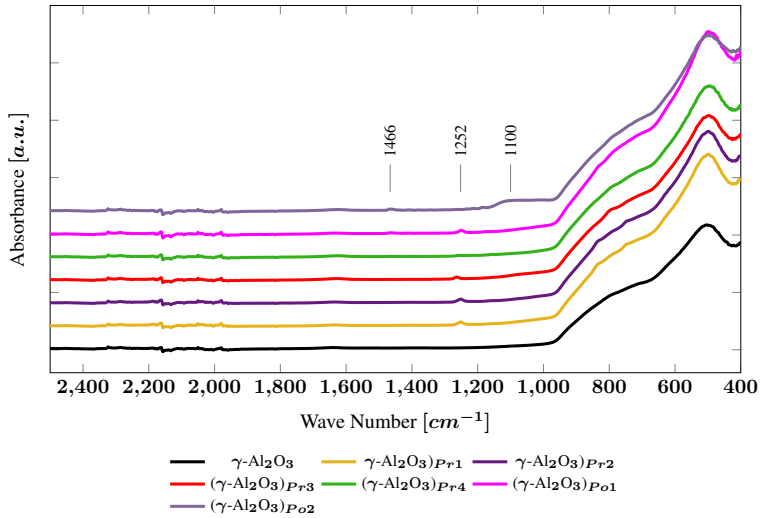

Figure 6.2: FT-IR spectra (2500-400 cm^{-1}) of surface modified supports.

Adsorption bands at 3430 and 1635 cm^{-1} were assigned to O-H stretching modes and H-O-H bending vibrations of the free and adsorbed water [6, 10]. Adsorption peaks at 2960, 2923 and 2853 cm^{-1} correspond to CH stretches of CH_3 groups. Peaks at 1466 and 1252 cm^{-1} correspond to bending and rocking vibration of C-H group respectively [6, 10]. Broad peak at 1100 cm^{-1} corresponds to *Si-O-Si* vibrations [5].

FT-IR spectra of modified supports indicated presence of hydrocarbon groups on the surface of all modified supports evident from peaks corresponding to CH_3 group as shown in Figure 6.1. As indicated in water absorption test, strongest surface modification effect was observed for (γ-$Al_2O_3)_{Po2}$ and (γ-$Al_2O_3)_{Po1}$. Relatively sharp peaks were observed for (γ-$Al_2O_3)_{Po2}$ as compared to (γ-$Al_2O_3)_{Po1}$, which is in agreement with the fact that OTCS is capable of multilayer formation. Broad peak at 1100 cm^{-1} corresponding to *Si-O-Si* vibrations confirms multilayers formation capability of OTCS. DMMeOS can only form monoloayer and correspondingly less alkyl groups are attached to the surface.

Methoxytrimethylsilane, chlorotrimethylsilane, dimethyldichlorosilane and chlorodimethyloctylsilane modified supports show relatively less sharp organic peaks indicating a lower extent of surface modification, which is in agreement with water absorption test.

Both Water absorption test and FT-IR analysis revealed successful surface modification of γ-Al_2O_3 with silanes although the extent of surface modification varied for different silanes.

6.1.1 Structure of Modified Supports

Table 6.2 shows BET surface area, pore size and pore volume of modified supports determined by N_2 adsorption respectively.

Table 6.2: Surface area, pore volume and pore size of modified supports calculated from N_2 adsorption

Catalyst	**BET Surface Area** (SA) [m^2/g]	**Pore Volume** (PV) [cm^3/g]	**Avg. Pore Dia.**[a] (PD) [nm]
(γ-Al_2O_3)	173	0.69	15.9
(γ-$Al_2O_3)_{Pr1}$	164	0.71	17.4
(γ-$Al_2O_3)_{Pr2}$	160	0.62	15.4
(γ-$Al_2O_3)_{Pr3}$	160	0.66	16.5
(γ-$Al_2O_3)_{Pr4}$	168	0.66	15.8
(γ-$Al_2O_3)_{Po1}$	166	0.63	15.3
(γ-$Al_2O_3)_{Po2}$	158	0.54	13.6

Calculation of pore size and pore volume were based on BJH desorption method.
[a] PD = 4(PV/SA).

Results indicate that surface modification leads to a decrease in BET surface area, pore volume and pore size. (γ-$Al_2O_3)_{Po2}$ experienced highest decrease of all modified samples which is attributed to OTCS capability of formation of multilayers leading to a higher surface modification.

6.2 Pre-modification Method

Surface modification of alumina with chlorotrimethylsilane, dichlorodimethylsilane, methoxytrimethylsilane and chlorodimethyloctylsilane yielded partially hydrophobic supports. These

supports were aqueous impregnated via pre-modification method. Thus these silane were termed as pre-modifying silanes and γ-Al_2O_3 supports modified by pre-modifying silanes were termed as pre-modified supports.

Hydrophobicity of pre-modified supports plays a vital role in aqueous impregnation. In order to retain hydrophobic characteristic after calcination, it is important that surface hydrophobic layers remain stable during calcination. Therefore in this section hydrophobicity and thermal stability analysis of pre-modified supports and pre-modified catalyst is performed. Subsequently effect of pre-modification on structure of catalyst, cobalt crystallite size, reducibility and dispersion was studied.

6.2.1 Hydrophobicity of Pre-Modified Supports

Thermal gravametric analysis of modified supports was carried out to find relative extent of surface modification of different silanes. Mass spectrum analysis of exhaust gases from TGA was performed for methane, silicon, chlorine, water and CO_2. Only Water and carbon dioxide peaks were observed at same temperatures indicating burning of surface alkylsilyl groups whereas methane, chlorine and silicon signals were not detected in any of the samples.

Figures 6.3, 6.4, 6.4 show the TGA profiles, derivative of TGA profile and ion current curves for water obtained from MS for pre-modified supports respectively. Mass loss occurred between 30-150 ^oC and 150-800 ^oC is mentioned on the curve in Figure 6.3.

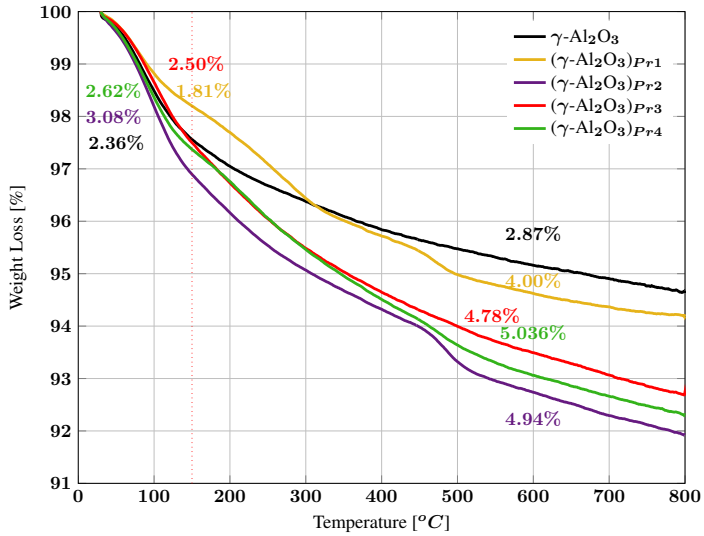

Figure 6.3: TGA profiles in O_2/N_2 for pre-modified supports.

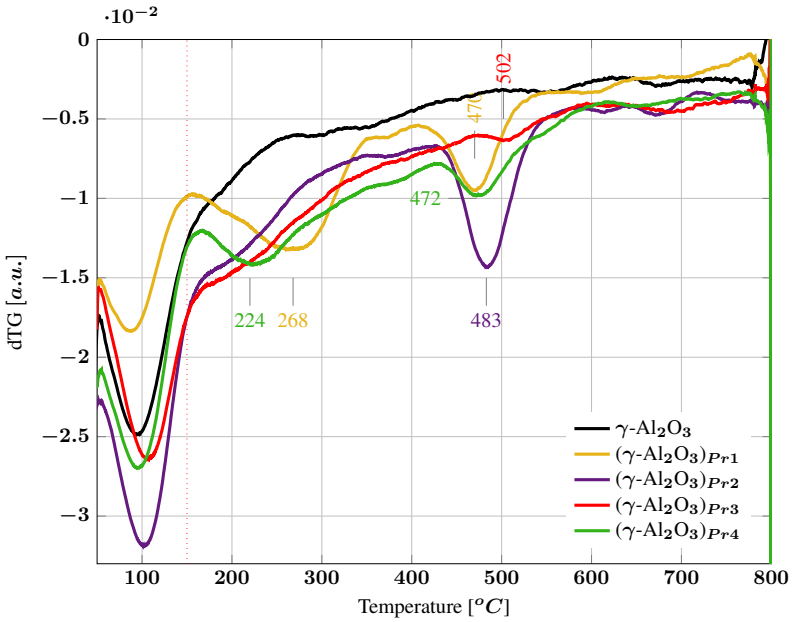

Figure 6.4: Derivative of TGA profiles in O_2/N_2 for pre-modified supports.

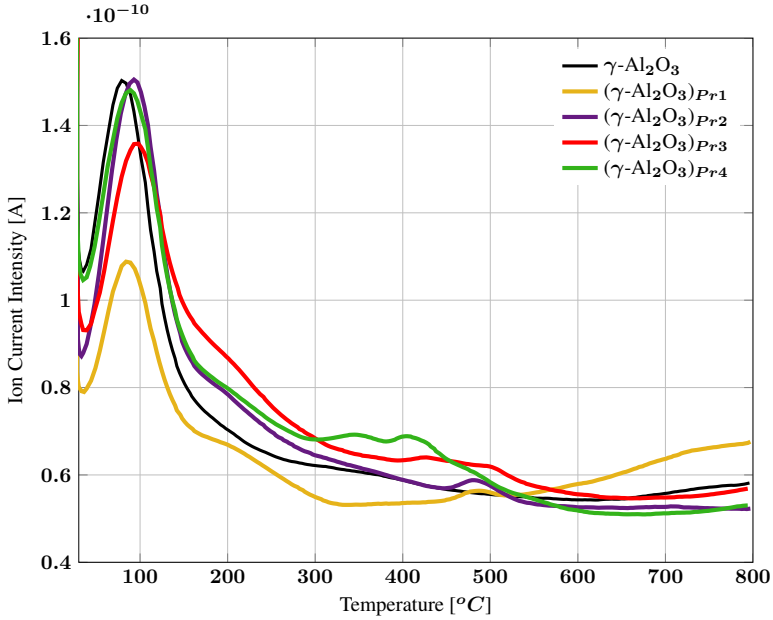

Figure 6.5: Ion current curves of water from MS for pre-modified supports.

Capel et al. [72] showed that initial mass loss due to desorption of water, during TGA can be used as an indirect measure of hydrophobicity. TGA was carried out in O_2/N_2 atmosphere and mass loss occurred between 30-150 ^oC, which is attributed to desorption of water was selected as an indirect measure of hydrophobicity.

Surface modified supports do not undergo any treatment after modification. Small quantities of unreacted silanes, solvent n-hexane and adsorbed water can be present. Solvent n-hexane and all pre-modifying silanes (except chlorodimethyloctylsilane) have boiling points less than 75 ^oC. In this research work, owing to the evaporation of unreacted species, initial mass loss cannot be taken as an absolute measure of hydrophobicity. Mass loss and ion current curves of water from MS were analyzed simultaneously to get an insight of hydrophobic nature.

Mass loss of pre-modified supports are tabulated in Table G.1 in Appendix G. During the temperature zone of 30-150 ^oC, mass loss follows the order

$$(\gamma\text{-}Al_2O_3)_{Pr1} < \gamma\text{-}Al_2O_3\ (\gamma\text{-}Al_2O_3)_{Pr3} < (\gamma\text{-}Al_2O_3)_{Pr4} < (\gamma\text{-}Al_2O_3)_{Pr2}$$

During the same temperature zone, peak of ion current curve of water follows the order as shown in Figure 6.5.

$$(\gamma\text{-}Al_2O_3)_{Pr1} < (\gamma\text{-}Al_2O_3)_{Pr3} < (\gamma\text{-}Al_2O_3)_{Pr4} < (\gamma\text{-}Al_2O_3)_{Pr2} < \gamma\text{-}Al_2O_3$$

Neglecting position of γ-Al_2O_3 in the trends, mass loss and peak height of water curve followed the same trend for pre-modified supports. $(\gamma\text{-}Al_2O_3)_{Pr1}$ showed less mass loss than γ-Al_2O_3 and the lowest water peak indicating that TMMeS modification has the most hydrophobic effect. Chlorosilanes modified samples ($(\gamma\text{-}Al_2O_3)_{Pr2-4}$) exhibited less intense water peaks than γ-Al_2O_3 but experienced more mass loss in comparison with γ-Al_2O_3. This implies that chloro-silane modified support were hydrophobic in comparison with γ-Al_2O_3 and extra mass loss was due to the evaporation of unreacted species present on the surface.

Among chlorosilanes modified samples, $(\gamma\text{-}Al_2O_3)_{Pr3}$ displayed the most hydrophobic behavior. Intrinsic ability of DMDCS to form multilayer enables it to yield more hydrophobic alumina in comparison with silanes capable of monolayer formation. $(\gamma\text{-}Al_2O_3)_{Pr2}$ shows almost the same height of water peak as γ-Al_2O_3 and more mass loss than γ-Al_2O_3. This indicates that TMCS modification has very little hydrophobic characteristics despite of its presence on the surface evident by higher mass loss than γ-Al_2O_3.

6.2.2 Thermal Stability of Pre-modified Supports

Thermal stability of pre-modified supports during calcination was studied using TGA in O_2/N_2 atmosphere for 150-800 ^oC temperature range. Figures 6.3, 6.4, 6.4 show the TGA profiles, derivative of TGA profile and ion current curves for water obtained from MS for pre-modified supports respectively.

As shown in Figure 6.4, $(\gamma\text{-}Al_2O_3)_{Pr1}$ shows the first minimum of differential curve at 268 ^oC. Mass loss in this temperature range was insignificant and water peak was not detected as well. Most probably, condensation or partial decomposition of alkylsilyl layer occured at this temperature. It is important to note that only hydrophobic groups get decomposed during calcination and silicon groups which replaced the surface hydroxyl groups were retained on the surface. $(\gamma\text{-}Al_2O_3)_{Pr3}$ showed most stable behavior as it

shows the lowest mass loss. This stable behavior was attributed to multilayer formation capability of DMDCS.

(γ-$Al_2O_3)_{Pr4}$ differential curve has a dip at 224 ^oC which corresponds to boiling point of DMOCS in range of 222-225 ^oC, as shown in Figure 6.4. Although mass loss in this region is not so significant but it gave the important indication that some unreacted DMOCS was present on the surface.

TGA analysis in relation to water analysis showed that burning of surface alkyl layer for all modified samples occurs above 300 ^oC. Therefore all the modifiers will be stable during calcination except for TMMeS which partially decomposed.

6.2.3 Surface Characterization of Pre-modified Catalysts

Pre-modified catalyst undergo calcination after surface modification. FT-IR analysis of pre-modified catalysts was performed to analyze the effect of calcination on hydrophobic surface alkylsilyl layer.

Figures 6.6 and 6.7 show the FT-IR spectra of pre-modified catalysts.

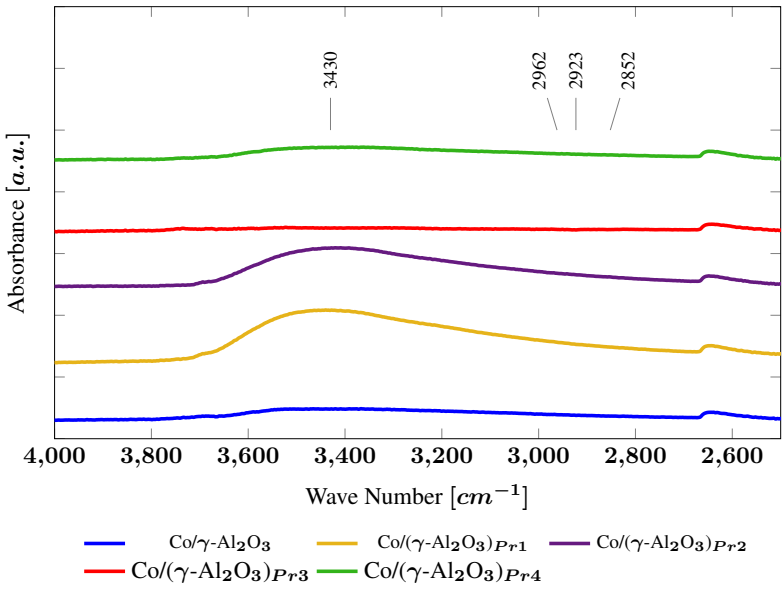

Figure 6.6: FT-IR spectra (4000-2500 cm^{-1}) of pre-modified catalysts.

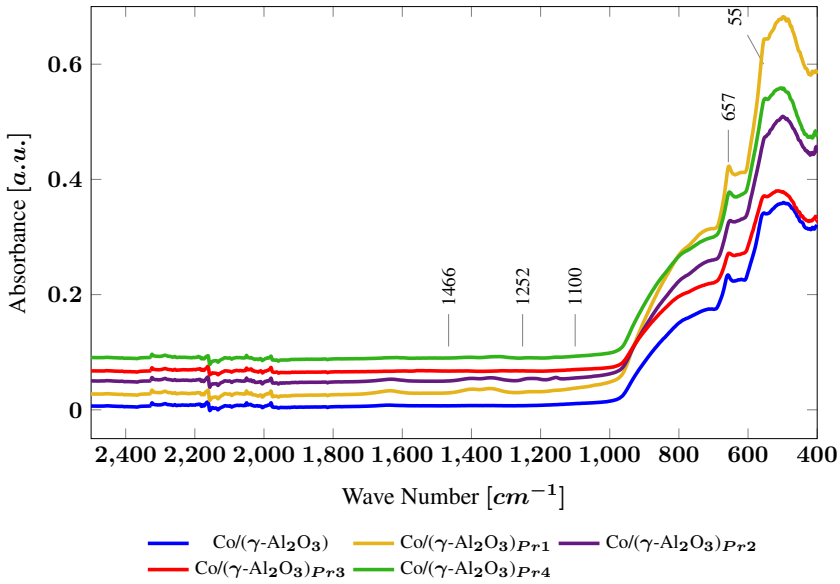

Figure 6.7: FT-IR spectra (2500-400 cm^{-1}) of pre-modified catalysts.

Adsorption bands at 657 and 555 cm^{-1} correspond to Co-O vibrations [5]. In contrast to pre-modified supports, pre-modified catalysts did not exhibit any organic peaks as shown in Figure 6.6. Ojeda et al. [8] also reported no peaks in FT-IR spectra of pre-modified catalysts. Pre-modified supports had not gone through any heat treatment after surface modification. Disappearance of organic peaks indicated that evaporation of unreacted species and partial decomposition of surface alkysilyl layer occured during calcination leaving behind little concentration of organic groups which were not detectable in FT-IR spectra.

6.2.4 Hydrophobicity of Pre-modified Catalysts

Hydrophobicity of pre-modified catalysts becomes a function of stability of hydrophobic alkylsilyl surface layer during calcination. Only TMMeS decomposition below calcination temperature was identified from TGA. Only decomposition of hydrocarbon groups was identified from TGA and silicon that substitutes the surface hydroxyl groups was retained on the surface.

Figures 6.8, 6.9, 6.10 show the TGA profiles, derivative of TGA profiles and ion current curves for water obtained from MS for pre-modified catalysts respectively.

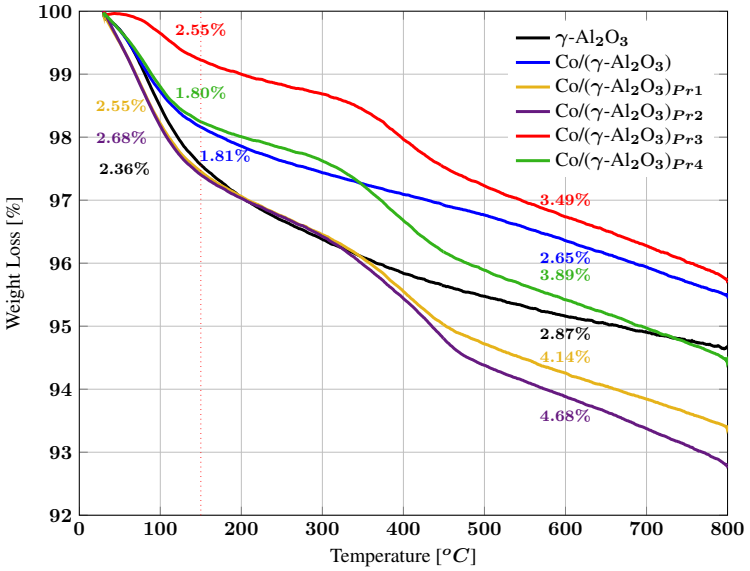

Figure 6.8: TGA profiles in O_2/N_2 for pre-modified catalyst

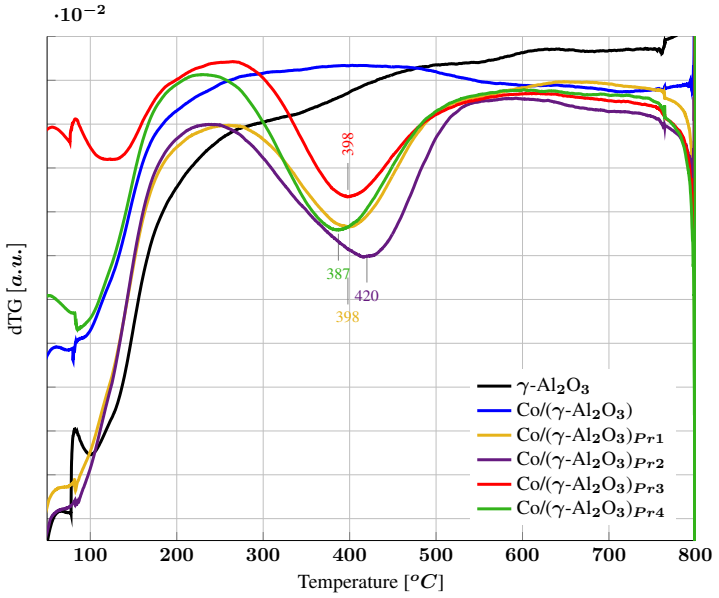

Figure 6.9: Derivative of TGA profiles in O_2/N_2 for pre modified supports

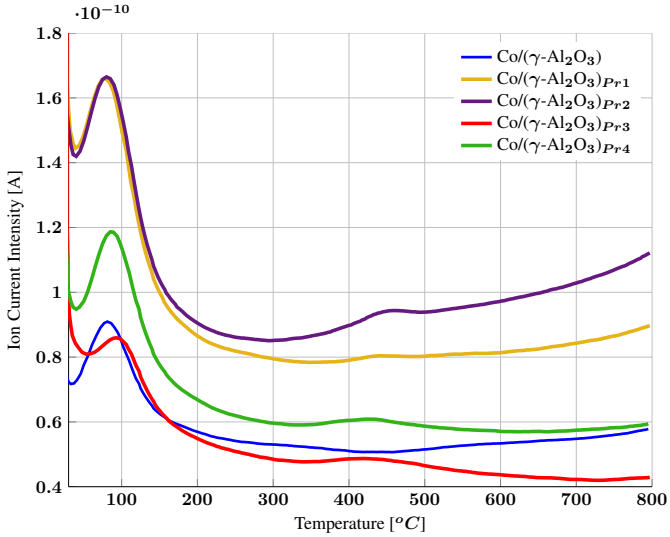

Figure 6.10: Ion current curves of water from MS for pre modified supports.

Hydrophobic effect of the organic groups retained on the surface was estimated by initial mass loss occurred between 30-150 ^oC. Mass losses are tabulated in Table G.2 in Appendix G and followed the order

$$\text{Co/}(\gamma\text{-Al}_2\text{O}_3)_{Pr3} < \text{Co/}(\gamma\text{-Al}_2\text{O}_3)_{Pr4} < \text{Co/}(\gamma\text{-Al}_2\text{O}_3) < \text{Co/}(\gamma\text{-Al}_2\text{O}_3)_{Pr1} < \text{Co/}(\gamma\text{-Al}_2\text{O}_3)_{Pr2}$$

Co/(γ-Al_2O_3)$_{Pr1}$ and Co/(γ-Al_2O_3)$_{Pr2}$ showed more mass loss than the reference catalyst. Higher mass loss of Co/(γ-Al_2O_3)$_{Pr1}$ confirmed the partial decomposition of TMMeS hydrophobic surface layer during calcination as indicated in TGA of support. Lowest surface TMCS modification potential has already been established as discussed in section 6.2.1 and confirmed by highest mass loss by Co/(γ-Al_2O_3)$_{Pr2}$.

Lowest mass loss of Co/(γ-Al_2O_3)$_{Pr3}$ is in agreement with multilayer formation capability of DMDCS and stability of surface hydrophobic layer during calcination.

6.2.5 Stability of Pre-modified catalyst

Pre-modified catalyst are reduced at 350 ^oC during dispersion measurement and Fischer-Tropsch synthesis. TGA analysis was used to get an indication of stability of modified surface layer at reduction temperature.

As shown in Figures 6.8, 6.9, 6.10, similar behavior was observed for all samples until 300 ^oC in terms of mass loss profile. This is due to the fact that all samples have gone through calcination at 300 ^oC previously. After 300 ^oC the mass loss profile becomes steep with significant mass loss in the temperature range of of 350-500 ^oC. A gradual mass loss up from 500-800 ^oC occurs attributed to the release of residual hydroxyl groups. Mass loss, derivative of mass loss and water curve confirm that decomposition of surface alkylsilyl layers occurs beyond 350 ^oC for all samples. Therefore it is confirmed that the

hydrophobic groups retained on the surface after calcination will not decompose during reduction conditions.

6.2.6 Structure of Pre-modified Catalysts

Table 6.3 shows BET surface area, pore size and pore volume of pre-modified catalyst determined by N_2 adsorption. BET surface areas of all samples are within the experimental accuracy range of BET (± 10). All samples (except Co/(γ-$Al_2O_3)_{Pr2}$) showed a higher BET surface area than the reference catalyst. This indicates that grafting of the surface with silanes resulted in roughening of the surface leading to a higher BET surface area.

Pore volume and average pore diameter of the modified samples decreased as a result of surface modification.

Table 6.3: Surface area, pore volume and pore size of pre-modified catalyst calculated from N_2 adsorption

Catalyst	**BET Surface Area** (SA) [m^2/g]	**Pore Volume** (PV) [cm^3/g]	**Avg. Pore Dia.**[a] (PD) [nm]
Co/γ-Al_2O_3	129	0.44	13.6
Co/(γ-$Al_2O_3)_{Pr1}$	133	0.42	12.5
Co/(γ-$Al_2O_3)_{Pr2}$	127	0.38	12.0
Co/(γ-$Al_2O_3)_{Pr3}$	139	0.37	10.7
Co/(γ-$Al_2O_3)_{Pr4}$	135	0.38	11.2

The calculation of pore size, surface area and pore volume are based on BJH desorption method.
[a] PD = 4(PV/SA).

6.2.7 Cobalt Crsytallite Size

Figure 6.11 shows the XRD profiles of pre-modified catalysts.

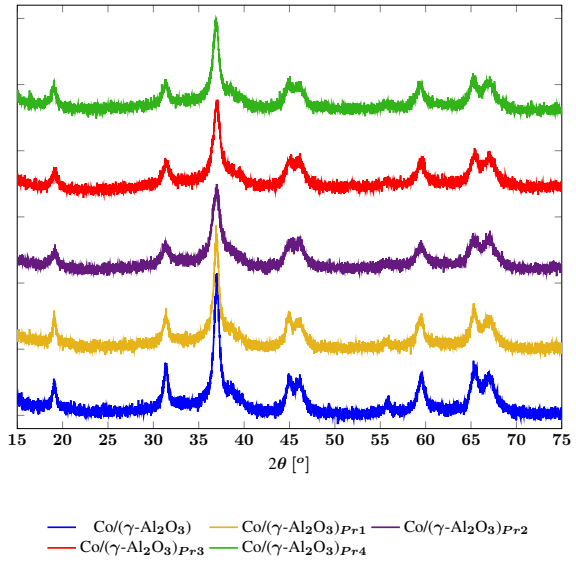

Figure 6.11: XRD profile of pre-modified catalysts

Table 6.4 shows cobalt crystallite sizes calculated from Scherrer equation and dispersion of cobalt calculated based on cobalt crystallite size.

Table 6.4: Cobalt crystallite sizes of pre-modified catalysts

Catalyst	**Crystallite Size [nm]**		**Dispersion**[b]
	Co_3O_4[a]	**Co**[o]	[%]
Co/(γ-Al_2O_3)	13.4	10.7	8.90
Co/(γ-Al_2O_3)$_{Pr1}$	13.4	10.7	9.00
Co/(γ-Al_2O_3)$_{Pr2}$[d]	8.60	6.90	13.9
Co/(γ-Al_2O_3)$_{Pr3}$	9.70	7.80	12.4
Co/(γ-Al_2O_3)$_{Pr4}$	10.7	8.60	11.2

[a] Calculated from the Scherrer equation

[b] Calculated using using D [%]= 96 / d_{Co^o}

Co/(γ-Al_2O_3)$_{Pr1}$ showed the same particle size as the reference catalyst. Chlorosilane modified catalysts (Co/(γ-Al_2O_3)$_{Pr2-4}$) showed a decrease in particle size. Cobalt particle size varied with the amount of chloro-silane present on the surface. Figure 6.13 in section 6.2.9 shows variation of crystallite size with amount of chloro-silane present on the surface. Co/(γ-Al_2O_3)$_{Pr2}$ showed highest mass loss and lowest cobalt crystallite size.

6.2.8 TPR Profiles of Pre-modified Catalysts

Figure 6.12 displayes the TPR profiles of pre-modified catalysts. During TPR of silane modified samples hydrogen is consumed for decomposition of surface alkylsilyl layer in addition to cobalt reduction. Due to this measurement of degree of reduction and reduction temperature of cobalt became difficult. Analysis of reduction profiles in assistance with TGA profiles facilitates understanding of the reduction behavior.

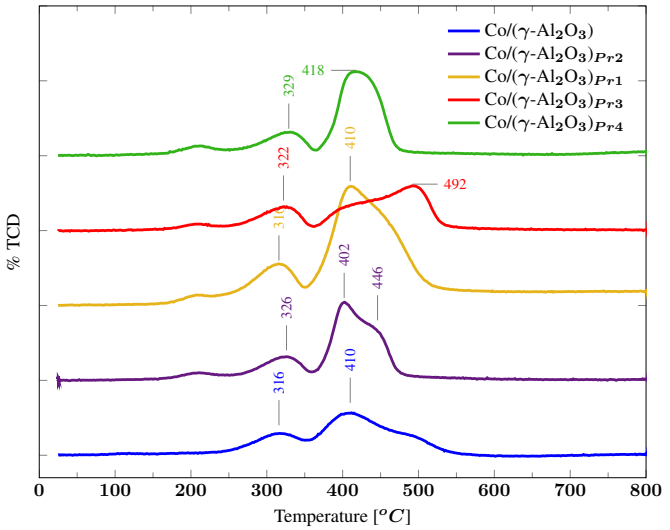

Figure 6.12: TPR profiles for pre-modified catalyts catalysts

Reference catalyst, Co/γ-Al_2O_3 showed reduction peaks at 316 ^oC and 410 ^oC for stepwise reduction of cobalt to metallic specie as shown in Figure 6.12 which is in agreement with literature [73].

Co/(γ-Al_2O_3)$_{Pr1}$ showed reduction peaks at exactly the same temperatures as reference catalyst. The second reduction peak is broad as it encapsulates the decomposition temperature of TMMeS.

For chloro-silane modified samples (Co/(γ-Al_2O_3)$_{Pr2-4}$), first reduction peak was shifted from 316 ^oC of reference catalyst to the range of 325 ^oC. Co/(γ-Al_2O_3)$_{Pr2}$ has first reduction peak at 326 ^oC, while the second peak is at 402 ^oC, but it shows a shoulder at 446 ^oC which corresponds to decomposition of the modifier as indicated in TGA Figure 6.9.

Co/(γ-Al_2O_3)$_{Pr3}$ shows first reduction peak at 322 ^oC, while the second peak is broad with a maximum at 492 ^oC. The second peak covers the decomposition temperature of DMDCS and second reduction step of cobalt to metallic specie. Co/(γ-Al_2O_3)$_{Po1}$ first peak occurs at 329 ^oC while second broad peak appears at 418 ^oC encapsulates the decomposition temperature of DMMeOS.

All chlorine modified samples have smaller cobalt crystallite sizes as compared to reference catalyst. Despite of the fact that difficulty of reduction increases with decrease

in the crystallite size [44, 74], insignificant increase in difficulty of reduction was observed, if hydrogen consumed for decomposition of surface hydrophobic layer is neglected. This can be attributed to decrease in cobalt support interaction due to surface modification.

6.2.9 Dispersion

Table 6.5 shows the dispersion of cobalt measured from hydrogen chemisorption.

Table 6.5: Dispersion of pre-modified catalyst measured from hydrogen chemisorption

Catalyst	Dispersion [%]
Co/(γ-Al_2O_3)	7.37
Co/(γ-Al_2O_3)$_{Pr1}$	8.36
Co/(γ-Al_2O_3)$_{Pr2}$[a]	2.22
Co/(γ-Al_2O_3)$_{Pr3}$	5.63
Co/(γ-Al_2O_3)$_{Pr4}$	3.49

[a] Average value of two independent dispersion runs

Cobalt is impregnated after surface modification of γ-Al_2O_3 for preparation of pre-modified catalysts and coverage of cobalt with surface modifier is unlikely. TMMeS modified catalyst, Co/(γ-Al_2O_3)$_{Pr1}$ exhibited enhanced dispersion than reference catalyst. This enhanced dispersion confirmed that increase in peak height in TPR profile was due to consumption of hydrogen in decomposition of alkylsilyl layer, not due to increased difficulty in reduction. TMMeS modification resulted in highest substitution of surface hydroxyl groups of γ-Al_2O_3 among all pre-modified samples. It can be inferred that this lower concentration of surface hydroxyl groups enhanced the dispersion but it needs further investigation.

In contrast, chlorosilanes pre-modified catalysts (Co/(γ-Al_2O_3)$_{Pr2-4}$) experienced a sharp decrease in dispersion. Experiments were performed twice for Co/(γ-Al_2O_3)$_{Pr2}$ to ensure accuracy of the results and average values are reported. Insignificant increase in difficulty of reduction was observed in TPR profiles therefore this decrease in dispersion of chloro-silane modified samples is attributed to the presence of chlorine. Borg et al. [75] observed similar sharp decrease in dispersion of Co/γ-Al_2O_3 catalysts upon introduction of chlorine impurity by post-impregnation of $CoCl_2.6H_2O$.

An inverse correlation is found between dispersion and amount of chloro-silane present on the surface of catalyst as shown in Figure 6.13. Numerical values are tabulated in Table G.3 in Appendix G. Total mass loss of modified catalyst is treated as an indirect measure of modifier present on the surface. Dispersions of the modified catalysts decreases with increase in amount of chloro-silane. Co/(γ-Al_2O_3)$_{Pr2}$ has the highest mass loss and exhibits the lowest dispersion.

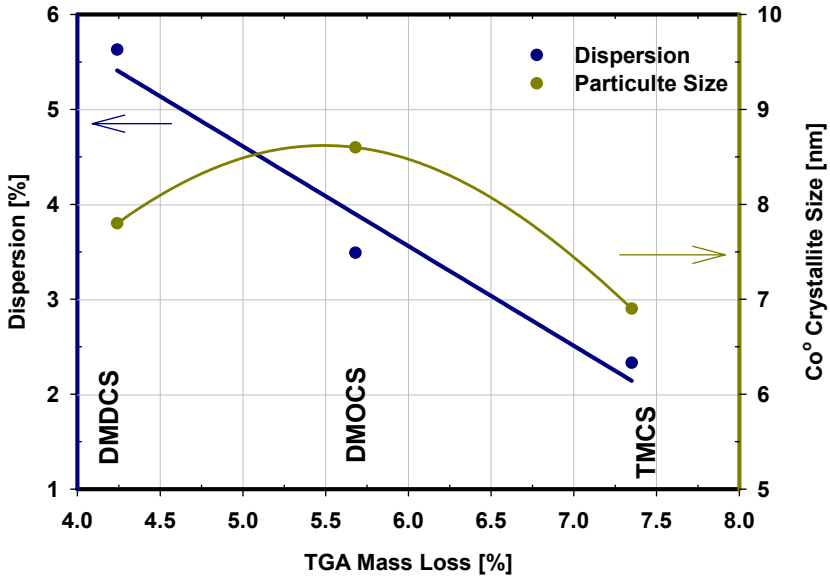

Figure 6.13: Correlation between cobalt dispersion, Co^{o} particulate size and amount of chlorosilane present on the surface

6.3 Post-modification Method

Surface modification with Methoxydimethyloctylsilane and trichlorooctylsilane yielded completely hydrophobic supports. This made aqueous impregnation impossible. Therefore, catalysts surface modified by these silanes were prepared by post-modification method. Hence these silanes were termed as post-modifying silanes and catalysts surface modified by these silanes were termed as post-modified catalysts.

Post-modifying silanes render completely hydrophobic surface therefore hydrophobicity analysis of post-modified catalysts was not required. Post-modified catalyst do not undergo any treatment after surface modification. Therefore thermal stability of post-modified catalyst is studied in this section. Subsequently effect of post-modification on structure of catalyst, cobalt crystallite size, reducibility and dispersion was studied.

6.3.1 Surface Characterization of Post-modified Catalysts

Figures 6.14 and 6.15 show the FT-IR spectra of post-modified catalysts. As post-modified catalysts do not undergo any heat treatment after surface modification so their FT-IR spectra remains same as those of post-modified supports as shown in Figures 6.1 and 6.2.

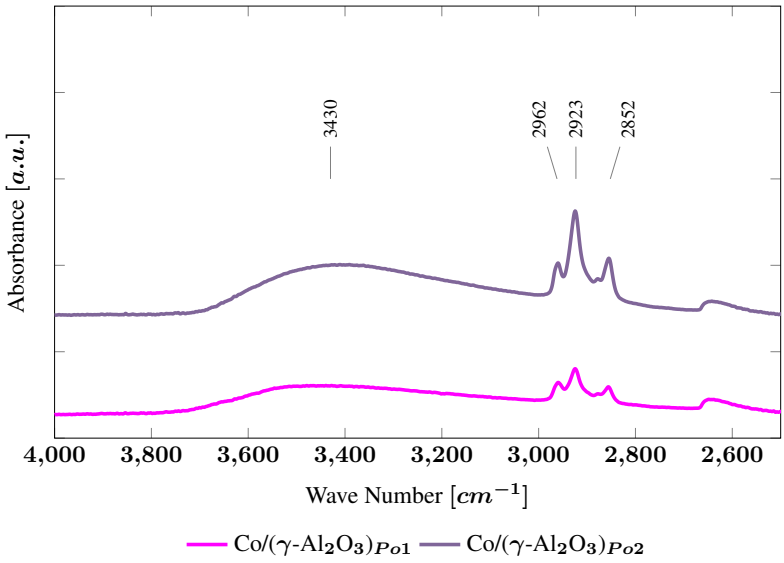

Figure 6.14: FT-IR spectra (4000-2500 cm^{-1}) of post-modified catalysts

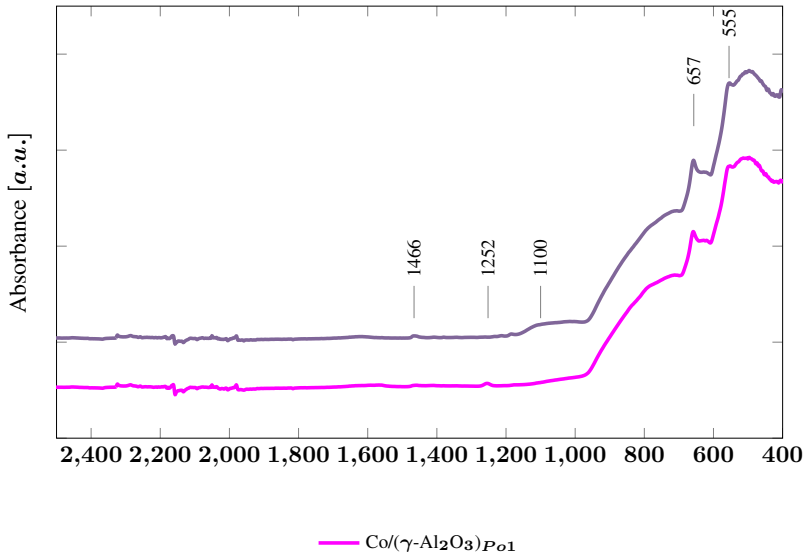

Figure 6.15: FT-IR spectra (2500-400 cm^{-1}) of post-modified catalysts

6.3.2 Thermal stability of post modified catalyst

Thermal stability of hydrophobic surface layer of post-modified samples at calcination and reduction temperatures was studied using TGA. Mass spectrum analysis of exhaust gases from TGA was performed for methane, silicon, chlorine, water and CO_2. Only water and carbon dioxide peaks were observed at same temperatures indicating burning of surface alkylsilyl groups whereas methane, chlorine and silicon signals were not detected in any of the samples.

Figures 6.16, 6.17, 6.18 show the TGA profiles, derivative of TGA profile and ion current curves for water obtained from MS for post-modified catalysts respectively.

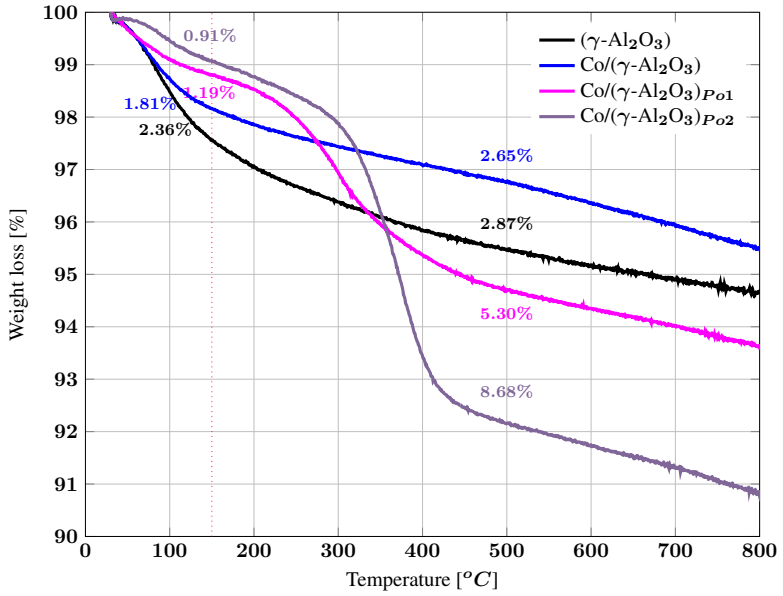

Figure 6.16: TGA profiles in O_2/N_2 for post-modified catalyst

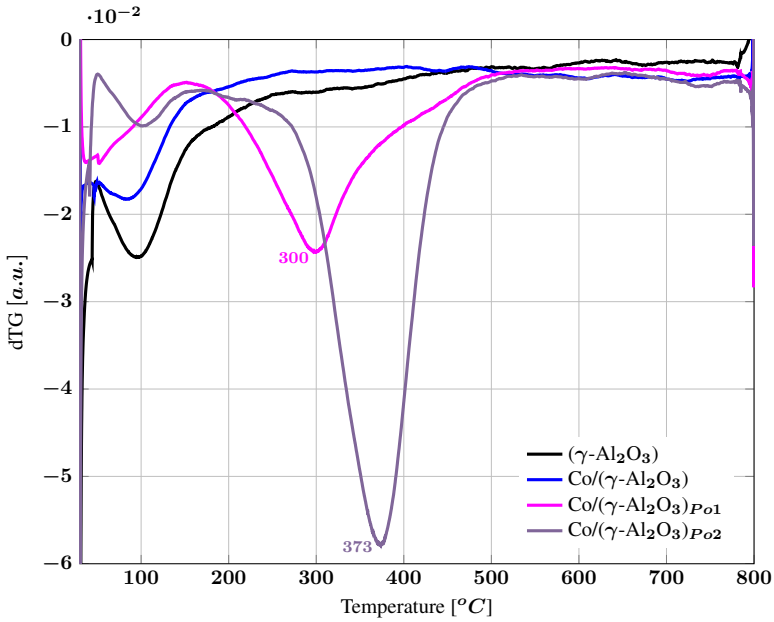

Figure 6.17: Derivative of TGA profiles in O_2/N_2 for post-modified supports

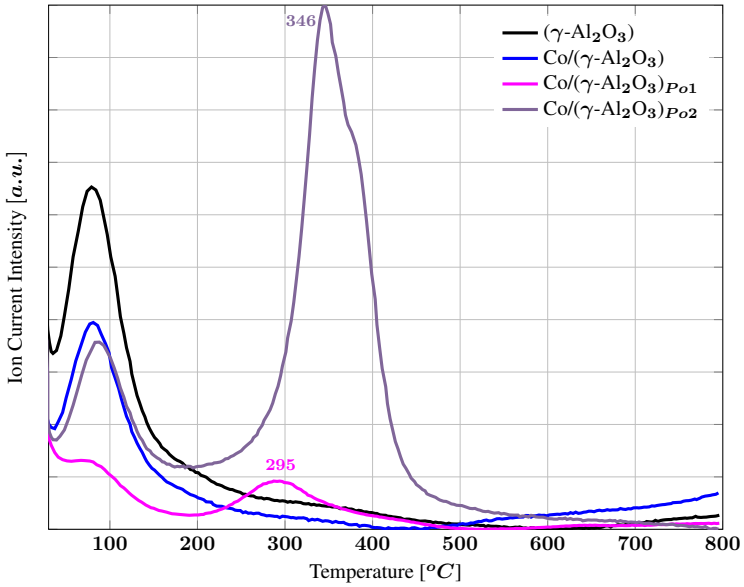

Figure 6.18: Ion current curves of water from MS for post-modified supports

TGA profile of Co/(γ-Al_2O_3)$_{Po1}$ showed a steep mass loss starting from 221 ^{o}C which is the boiling point of DMMeOS indicating that unreacted DMMeOS was present in the sample. A mass loss of 2.5 % occurs in 200-350 ^{o}C region with a dip of differential curve at 300 ^{o}C. Water peak appears at 295 ^{o}C. This indicates that decomposition of the surface alkyl groups occurs below calcination and reduction temperatures.

Boiling point of OTCS is 233 ^{o}C but Co/(γ-Al_2O_3)$_{Po1}$ did not show any significant mass loss at this temperature. It indicates that negligible amount of unreacted OTCS and n-hexane were present in the sample. TGA curve showed stable behavior until 300 ^{o}C with a gradual mass loss. However TGA curve showed a steep slope with a mass loss of 5% in 300-400 ^{o}C region. Derivative of the mass loss curve showed a dip at 373 ^{o}C and ion current curve of water in Figure 6.18 showed peak at 346 ^{o}C with a secondary shoulder at 374 ^{o}C. This indicates that much of the decomposition occurs in the temperature zone of 300-400 ^{o}C. This zone includes the reduction temperature i.e 350 ^{o}C implying that partial decomposition of OTCS surface layer will occur during reduction.

A gradual mass loss was shown by both samples until 800^{o}C which is attributed to the removal of residual *-OH* groups.

6.3.3 Structure of post-modified catalysts

Table 6.6 shows BET surface area, pore size and pore volume of post-modified catalysts determined by N_2 adsorption respectively.

Table 6.6: Surface area, pore volume and pore size of post-modified catalysts calculated from N_2 adsorption

Catalyst	**BET Surface Area** (SA) [m^2/g]	**Pore Volume** (PV) [cm^3/g]	**Avg. Pore Dia.**[a] (PD) [nm]
Co/γ-Al_2O_3	129	0.44	13.6
Co/(γ-Al_2O_3)$_{Po1}$	117	0.39	13.3
Co/(γ-Al_2O_3)$_{Po2}$	112	0.35	12.5

The calculation of pore size, surface area and pore volume are based on BJH desorption method.
[a] PD = 4(PV/SA).

Post silylation resulted in a significant decrease in surface areas for both samples. The BET surface area decreased from 129 m^2/g for reference catalyst to 117 m^2/g and 112 m^2/g for Co/(γ-Al_2O_3)$_{Po1}$ and Co/(γ-Al_2O_3)$_{Po2}$ respectively. A parallel decrease in pore volume was also observed. Similar decrease in surface area and pore volume was observed by Ojeda et. al and Capel Sanchez for silane modified silica support [8, 72].

6.3.4 Cobalt crsytallite Size

Figure 6.19 shows the XRD profiles of catalysts.

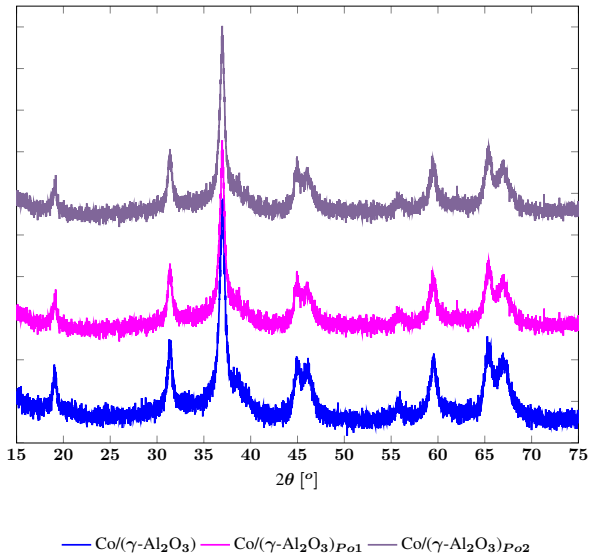

Figure 6.19: XRD profile of post-modified catalysts

Cobalt particulate sizes calculated from Scherrer equation and dispersion of cobalt calculated based on cobalt crystallite size are reported in Table 6.7.

Table 6.7: Cobalt crystallite sizes of post-modified catalysts

Catalyst	**Crystallite Size [nm]**		**Dispersion**[b]
	Co_3O_4[a]	**Co^o**	[%]
Co/(γ-Al_2O_3)	13.4	10.7	8.90
Co/(γ-Al_2O_3)$_{Po1}$	14.6	11.6	8.20
Co/(γ-Al_2O_3)$_{Po2}$[c]	14.6	11.7	8.20

[a] Calculated from the Scherrer equation according to the diffraction peak of Co_3O_4

[b] Calculated using Co^o crystallite size using D [%]= 96 / d_{Co^o}

[c] Average value of two independent dispersion results

Cobalt crystallite sizes of post modified catalysts are comparable with the reference catalyst, keeping in view the experimental accuracy of ± 1 nm. This is because impregnation was carried before surface modification, therefore it was unlikely that crytallite sizes will be effected by modification. This observation is in agreement with the literature [5, 8].

6.3.5 TPR Profiles of Post-modified Catalysts

Figure 6.20 shows the TPR profiles of post-modified catalysts.

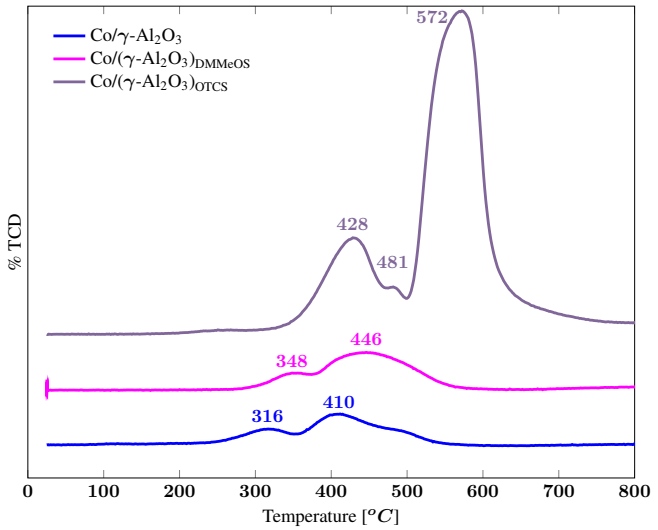

Figure 6.20: TPR profiles for post modified catalyts catalysts

For methoxydimethyloctylslane modified catalyst, Co/(γ-Al_2O_3)$_{Po1}$ broad reduction peaks occur at 348 ^{o}C and 446 ^{o}C. Despite lower decomposition temperature of DMMeOS surface alkylsilyl layer, there is a significant increase in difficulty of reduction as both reduction peaks are shifted to a higher temperature.

For trichloroctylsilane modified catalyst, Co/(γ-Al_2O_3)$_{Po2}$, two significant peaks were observed at 428 ^{o}C and 572 ^{o}C with a small shoulder at 481 ^{o}C. From TGA, the water peak was at 346 ^{o}C and max mass loss at 370 ^{o}C. First broad reduction peak includes the surface layer decomposition. The second shoulder at 481 ^{o}C and very high second reduction peak at 572 ^{o}C indicate significant increase in difficulty of reduction. This significant increase in difficulty of reduction of Co/(γ-Al_2O_3)$_{Po2}$ is explained by the multilayers formation capability of OTCS, which are three dimensional networks on the surface. After decomposition of surface hydrocarbon groups, distorted network of silicon keeps the active cobalt sites blocked which prohibits cobalt reduction.

Decomposition of organic group can be difficult in hydrogen atmosphere as compared to burning in oxidizing atmosphere. This can also contribute to increase in difficulty of reduction. Post-modification clearly increases the difficulty in reduction which is contrary to Ojeda et al. observation of insignificant change in reduction behavior [8].

6.3.6 Dispersion

Table 6.8 shows the dispersion of cobalt measured from hydrogen chemisorption.

Table 6.8: Dispersion of post-modified catalyst measured from hydrogen chemisorption

Catalyst	Dispersion [%]
Co/(γ-Al_2O_3)	7.37
Co/(γ-Al_2O_3)$_{Po1}$	5.41
Co/(γ-Al_2O_3)$_{Po2}$[d]	0.66

In post-modification method, surface modification of the catalyst was performed after impregnation of cobalt. This resulted in coverage of active metal with hydrophobic alkylsilyl layer. Dispersion becomes a function of stability of the surface layer at reduction temperature. Silicon network retained on the surface after decomposition of organic groups dictates the dispersion.

Lower dispersion of methoxydimethyloctylslane modified catalyst, Co/(γ-Al_2O_3)$_{Po1}$ is attributed to increase in difficulty of reduction. Decomposition of organic groups Co/(γ-Al_2O_3)$_{Po1}$ occurs below reduction temperature, as evident from TGA. DMMeOS can only form monolayer so less silica groups react to the surface and after decomposition of organic group their shielding effect is lower. Therefore relatively higher dispersion is shown by Co/(γ-Al_2O_3)$_{Po1}$ as compared to Co/(γ-Al_2O_3)$_{Po2}$.

Negligible dispersion of Co/s-(γ-Al_2O_3)$_{Po2}$ is explained by significant increase in difficulty of cobalt reduction.

6.4 Comparison of Surface Modification Potential of Different Silanes

Identical experimental conditions and concentrations of modifier solutions were used for surface modification of γ-Al_2O_3 and Co/s-(γ-Al_2O_3). Hydrophobic characteristics varied for different silanes depending upon the chemical structure and reactivity of the silanes at modification conditions.

Trichloroctylsilane and methoxydimethyloctylsilane yielded completely hydrophobic γ-Al_2O_3 support indicating significantly higher surface modification potentials. Other silanes yielded partially hydrophobic supports with surface modification potential of silanes decreasing in the order TMMeS $>$ DMDCS $>$ DMOCS $>$ TMCS as evident from TGA analysis discussed in section 6.2.1.

Methoxysilanes displayed higher surface modification potential as compared to their chlorosilanes counter parts. In case of methoxydimethyloctylsilane and chlorodimethyloctyl silane, former one yielded completely hydrophobic $\gamma - Al_2O_3$ while modification with later one resulted in partial surface modification. In case of methoxytrimethylsilane and chlorotrimethylsilane, higher potential of TMMeS was evident from the higher hydrophobic characteristic.

6.5 Fischer-Tropsh Synthesis

Table 6.9 shows the activity and selectivity results for catalytic run performed in Fischer-Tropsch rig operated at 210 ^{o}C and 20 bar and H_2/CO =2.1.

Table 6.9: Activity & selectivity of surface modified catalysts

Catalyst	rCO Initial[a]	CO Conversion	STY[b]	Selectivities [%]			O/P ratio
	$[molCO/g_{cat}.h]$	[%]	$[s^{-1}]$	CH_4	C_2-C_4	C_{5+}	C3=/C3-
Co/(γ-Al_2O_3)	0.0577	50.2	0.0529	7.43	6.88	85.69	2.5
Co/(γ-Al_2O_3)$_{Pr1}$	0.0719	49.3	0.0656	9.01	5.84	85.15	1.4
Co/(γ-Al_2O_3)$_{Pr2}$	0.0796	50.2	0.0468	7.97	6.04	85.99	1.7
Co/(γ-Al_2O_3)$_{Pr3}$	0.0675	49.8	0.0446	7.83	6.01	86.16	1.8
Co/(γ-Al_2O_3)$_{Pr4}$	0.0621	50.4	0.0453	8.78	6.45	84.77	1.8
Co/(γ-Al_2O_3)$_{Po1}$	0.0469	49.9	0.0466	8.7	8.25	83.04	1.9
Co/(γ-Al_2O_3)$_{Po2}$	0.0232	53.7	0.0231	7.15	6.99	85.86	2.2

[a] Initial rate of reaction calculated at 20 hours of service

[b] STY calculated on the basis of dispersion calculated from XRD

Contrary to low dispersion of chlorosilane pre-modified catalysts Co/(γ-Al_2O_3)$_{Pr2-4}$, initial rates of reactions of chlorosilanes modified samples are quite high. This implies that the dispersion of chlorosilanes calculated from hydrogen chemisorption is apparently low. Therefore dispersion that is calculated based upon cobalt crystallite size and site time yield (STY) based on that dispersion is used for modified samples to ensure consistency of comparison.

Apparent low dispersion was only exhibited by chlorosilane modified samples. TMMeS modified sample Co/(γ-Al_2O_3)$_{Pr1}$ showed actual dispersion. Dispersion of post-modified samples calculated from cobalt crystallite size does not take into account the coverage of cobalt sites by surface alkylsilyl layer and results in higher apparent dispersion. A comparison of site time yield based on hydrogen chemisorption and cobalt crystallite size for methoxytrimethylsilane and post-modified catalyst is shown in Table 6.10.

Table 6.10: STY comparison of post-modified and methoxytrimethylsilane pre-modified catalysts

Catalyst	STY (H_2 Chemisorption) $[s^{-1}]$	STY (Co Crystallite Size) $[s^{-1}]$
Co/(γ-Al_2O_3)	0.064	0.053
Co/(γ-Al_2O_3)$_{Pr1}$	0.070	0.066
Co/(γ-Al_2O_3)$_{Po1}$	0.071	0.047
Co/(γ-Al_2O_3)$_{Po2}$	0.253	0.023

6.5.1 Post-Modified Catalysts

STY of post-modified samples calculated from hydrogen chemisorption gives an insight to actual dispersion and is used for comparison of activity of post-modified samples as shown in Table 6.10.

Methoxydimethyloctylslane modified catalyst, Co/(γ-Al_2O_3)$_{Po1}$ has a higher STY and lower C_{5+} selectivity than the reference catalyst. This higher STY is attributed to the lower concentration of surface hydroxyl groups. Steric hindrance of hydrocarbon groups of methoxydimethyloctylslane can be a probable reason of lower C_{5+} selectivity.

Co/(γ-Al_2O_3)$_{Po2}$ showed very low Fischer-Tropsch activity in agreement with high difficulty in reduction and negligible cobalt dispersion. C_{5+} selectivity is approximately similar as the reference catalyst but it is important to note that C_{5+} is reported at a higher CO conversion level i.e 50.4 %. Trichlorooctylsilane yields the most hydrophobic catalyst but contrary to Co/(γ-Al_2O_3)$_{Po1}$, very low STY is observed. It seems that surface modification with OTCS surpasses the optimum extent of surface modification required for enhanced Fischer-Tropsch activity.

Olefin to paraffin ratio (O/P ratio) of both post-modified samples was lower than for the reference catalyst.

6.5.2 Pre-Modified Catalysts

As discussed dispersions of chlorosilane modified samples Co/(γ-Al_2O_3)$_{Pr2-4}$ are apparently less than actual dispersions. Therefore activities of pre-modified catalysts are compared on the basis of STY calculated from cobalt crystallite sizes.
Selectivities to C_{5+} hydrocarbons of all pre-modified catalysts were similar as the reference catalyst except Co/(γ-Al_2O_3)$_{Pr4}$ keeping in view the experimental accuracy of $\pm$0.5 %.

Methoxytrimethylsilane modified catalyst, Co/(γ-Al_2O_3)$_{Pr1}$ has higher STY (both hydrogen and cobalt particle size based) than the reference catalyst. Among all pre-modified catalysts, Co/(γ-Al_2O_3)$_{Pr1}$ also has lowest O/P ratio and highest CH_4 selectivity. As discussed, methoxytrimethylsilane had the highest surface modification effect which means that it replaced the most surface hydroxyl groups. Higher STY of Co/(γ-Al_2O_3)$_{Pr1}$ is attributed to lower concentration of surface hydroxyl groups. This rules out the assumption that Co/α-Al_2O_3 has higher C_{5+} selectivity than Co/γ-Al_2O_3 catalyst due to lower surface hydroxyl groups [30]. In fact, surface modification with methoxy-silanes resulted in similar increase in STY for both pre-modified Co/(γ-Al_2O_3)$_{Pr1}$ and post-modified Co/(γ-Al_2O_3)$_{Po1}$ catalysts.

All chlorosilanes modified catalysts Co/(γ-Al_2O_3)$_{Pr2-4}$ showed lower STY than the reference catalyst. In case of chloro-silanes modified catalysts it was difficult to analyze the effect of surface modification alone as cobalt crystallite size changed for all samples and dispersion measurement from hydrogen chemisorption was apparently inaccurate. Effect of chlorine on particle size and dispersion needs further investigation.

Effect of particle size on STY and C_{5+} selectivity

Bezemer [76] investigated the effect of cobalt particle size on acitivity and selectivity of cobalt catalyst supported on carbon nanofibers. They found that site-time yield (STY) for CO hydrogenation was independent of cobalt particle size for catalysts with sizes larger 8 nm (FT synthesis at 35 bar). C_{5+} selectivity increased with cobalt particle size upto 10 nm and became constant for larger particles. It is important to note that C_{5+} was reported

at CO conversion varying from 60-80% and it is demonstrated that C_{5+} varies with CO conversion [30].

Borg [30] observed very small variation in turn over frequency (TOF) with particle size for cobalt catalyst supported on γ-Al_2O_3. C_{5+} selectivity increased with particle size with a maximum selectivity at 7-8 nm and became constant for larger particle sizes. Similar selectivity results were obtained by Rane et al. [46] for cobalt supported on θ–Al_2O_3 and δ-Al_2O_3.

Pre-modification with chloro-silane resulted in lower cobalt crystallite sizes. Figure 6.21 shows plot of cobalt crystallite size against site-time yield and C_{5+} selectivity. Co/(γ-$Al_2O_3)_{Pr2}$ has smallest cobalt crystallite size of 6.90 nm which is at the threshold of maximum C5+ selectivity and site-time yield. Contrary to Bezemer, Borg and Rane an abrupt variation exists between cobalt crystallite size, STY and C_{5+} selectivity. This is due to the fact that in addition to particle size surface structure of γ-Al_2O_3 has changed. It is already established that supports play an important role in FT synthesis.

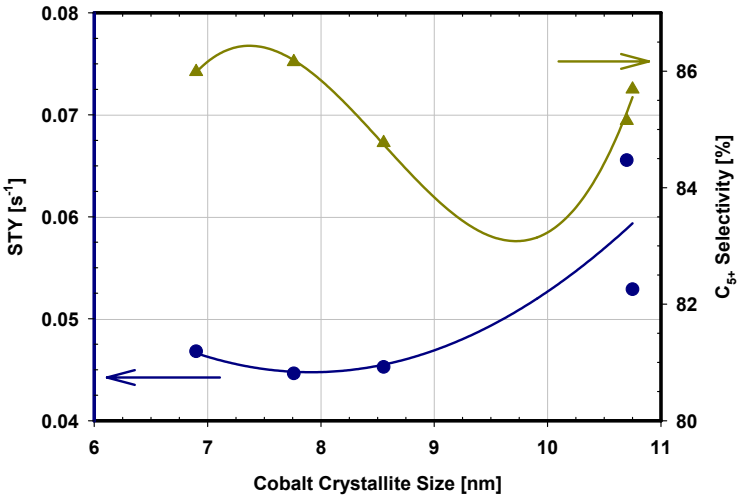

Figure 6.21: Catalytic stability of the post modified samples

Olefin/paraffin ratio

All modified samples have a lower olefin/paraffin ratio than the reference catalyst. This can be attributed to hydrophobicity. Iglesia [2] showed that addition of water at moderate partial pressure increase site-time yield, C_{5+} selectivity and olefin/paraffin ratio for Co/TiO_2 and Co/SiO_2 catalysts. Storsæter [26] observed similar increase in C_{5+} selectivity and olefin/paraffin ratio for Co/Al_2O_3 catalyst. Irreversible chain termination by hydrogen addition and secondary hydrogenation pathways is inhibited by water addition leading to a higher O/P ratio [2]. This implies that hydrophocity will lead to a lower O/P

ratio. Results in current research work are in agreement with this observation. All samples experienced similar reduction in O/P ratio with Co/(γ-Al_2O_3)$_{Po2}$ as an exception.

Addition of water at moderate partial pressure during FT synthesis, increases C_{5+} selectivity which means that hydrophobicity induced in catalyst by surface modification will decrease C_{5+} [29]. Relatively minor variations in C_{5+} selectivities of pre-modified catalysts is observed.

Variation in product selectivity

Figure 6.22 shows plot of C_{5+} selectivity against CH_4 and C_2-C_4 selectivitites. It has been shown that CH_4 selectivity decreases linearly with increasing C_{5+} selectivity [46]. In contrast a diversified behaviour is shown by surface modified catalysts.

Figures 6.21 and 6.22 suggest that grafting of silanes onto the surface of the catalyst interfere with mechanism of chain propagation and also termination evident by varied change in O/P ratio independent of the effect of particle size. This needs further investigation for complete understanding.

It is difficult to analyze effect of hydrophobicity on C_{5+} selectivity as several variables i.e particle size, surface structure of support, steric hindrance of surface hydrophobic groups and effect of chlorine are changing simultaneously.

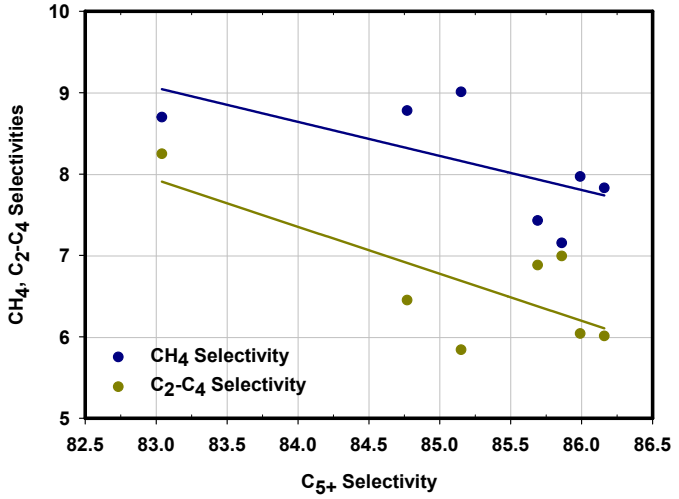

Figure 6.22: Catalytic stability of the post modified samples

Chapter 7

Conclusion

This research work focused on investigating the effect of silane modification on activity and selectivity of Co.Re/γ-Al_2O_3 Fischer-Tropsch catalysts. Catalysts with 20 wt % cobalt promoted with 0.5 wt% rhenium were prepared by one step aqueous incipient wetness impregnation. Surface modification was carried out by two methods, pre-modification: silane modification of γ-Al_2O_3 prior to cobalt impregnation and post-modification: silane modification of catalyst after cobalt impregnation. Catalysts were characterized by hydrogen chemisorption, nitrogen adsorption, TPR, TGA, FT-IR and XRD. Activity and selectivity of catalysts have been determined in a fixed bed reactor at 20 bar, 210 ^oC and H_2/CO = 2.1.

Six silanes, methoxytrimethylsilane (TMMeS), chlorotrimethylsilane (TMCS), dichlorodimethylsilane (DMDCS), chlorodimethyloctylsilane (DMOCS), methoxydimethyloctylsilane (DMMeS) and trichloroctylsilane (OTCS), differing with respect to numbers and types of organic groups and active groups, were used for surface modification. Silylation of γ-Al_2O_3 results in substitution of surface hydroxyl groups with hydrophobic organic groups connected to surface via $\equiv$*Si-O-Al* bond. Surface modified catalysts were compared with un-modified reference catalyst.

Analytical hydrophobicity test via water absorption and FT-IR spectra of silane modified alumina supports revealed successful modification of surface with DMMeS and OTCS yielding completely hydrophobic alumina support. Among partially hydrophobic supports, TMMeOS modified support had the most hydrophobic characteristics.

Most promising results were displayed by catalyst pre-modified with TMMeS, Co/(γ-$Al_2O_3)_{Pr1}$. It had similar cobalt crystallite size as reference catalyst. Insignificant change in difficulty of reduction was observed but dispersion increased to 8.36 % as compared to 7.37 % for reference catalyst. TGA suggested that Co/(γ-$Al_2O_3)_{Pr1}$ catalyst experienced partial decomposition of surface hydrocarbon groups. TMMeS pre-modification had the most positive influence on FT activity with similar C_5+ selectivity and increase in STY to 0.071 s^{-1} in comparison with 0.064 s^{-1} for reference catalyst, probably as a consequence of substitution of surface hydroxyl groups with silane inducing an hydrophobicity to the surface keeping in view that TMMeS modification resulted in highest substitution

of surface hydroxyl groups among pre-modifying silanes.

Other three pre-modifying silanes: TMCS, DMDCS, DMOCS contained chlorine as an active group and corresponding pre-modified catalysts Co/(γ-Al_2O_3)$_{Pr2-4}$ observed a decrease in cobalt crystallite size in comparison with the reference catalyst. Dispersion of Co/(γ-Al_2O_3)$_{Pr2-4}$ catalysts measured from hydrogen chemisorption was apparently lower than actual cobalt dispersion. Both these effects were attributed to the presence of chlorine and further investigation is needed for complete understanding. However a positive correlation was observed between cobalt crystallite size and amount of chlorosilane present on the surface. Despite of smaller cobalt cyrtallite size, insignificant change in reducibility was observed, probably due to lower cobalt support interactions as a result of surface modification. TG suggested that Co/(γ-Al_2O_3)$_{Pr2-4}$ catalysts remain stable during calcination and reduction. Co/(γ-Al_2O_3)$_{Pr2-4}$ catalysts observed relatively small change in C_{5+} selectivity but STY decreased significantly with highest decrease for DMOCS modified catalyst, having STY of 0.0453 s^{-1} in comparison with 0.064 s^{-1} for reference catalyst.

Post-modification of reference catalyst with DMMeS and OTCS to produce Co/(γ-Al_2O_3)$_{Po1}$ and Co/(γ-Al_2O_3)$_{Po2}$ catalysts respectively resulted in coverage of cobalt active species. Although TGA suggested that both catalysts undergo partial decomposition of hydrocarbon groups but remaining silica network keeps the surface blocked leading to a significant increase in difficulty of reduction and very low cobalt dispersion. Both Co/(γ-Al_2O_3)$_{Po1-2}$ catalysts had similar cobalt crystallite sizes and lower dispersions than reference catalyst with Co/(γ-Al_2O_3)$_{Po2}$ having a negligible dispersion of 0.66 % as compared to 7.37 % dispersion of reference catalyst, attributed to the multilayer formation capability of OTCS. Correspondingly Co/(γ-Al_2O_3)$_{Po2}$ had negligible FT activity.

Olefin/Paraffin ratio decreased for all modified samples suggesting that surface modification changes mechanism of chain growth and termination.

Methoxy-silanes exhibited higher surface modification potentials than corresponding chloro-silanes and a positive effect of methoxy-silanes modification on the activity of catalysts was ascribed to hydrophobicity induced by surface modification. Effect of surface modification with chlorosilane on dispersion, cobalt crystallite size and activity of catalysts need further investigation.

Chapter 8

Further Research Work

The project work has revealed that silane modification affects the activity and selectivity of Co/(γ-Al_2O_3) Fischer-Tropsch catalysts. Modification with methoxy-silanes had positive effect on activity of Co/γAl_2O_3 catalysts, whereas modification with chloro-silanes resulted in a decrease in activity of the catalysts. Also effect of chloro-silane modification on cobalt dispersion and crystallite size was not clearly understood.

In this research work, successful surface modification of γ-Al_2O_3 with silanes was confirmed but quantitative extent of modification was not calculated i.e how many surface hydroxyl groups have been substituted. Furthermore, all samples were modified at identical experimental conditions but due to difference in reactivities of silanes, surface modification to different extents was anticipated. It is proposed for future work to calculate the extent of modification and modify all samples to a similar extent of modification. This will enable a comprehensive comparison between samples modified with different silanes.

Effect of chloro-silane modification can be investigated by gradually increasing the concentration of modifier/n-hexane solution and observing effect on cobalt dispersion and crystallite size as amount of chlorine increases.

It is suggested to use mass spectrometer coupled with TPR to analyze off gases and also measure degree of reduction for each sample. More advanced characterization techniques like X-ray Fluorescence and Transmission electron microscopy (TEM) can be used to identify the surface phenomena occurring during the surface modification.

Bibliography

[1] E. Iglesia, S. L. Soled, R. A. Fiato, Fischer-Tropsch synthesis on cobalt and ruthenium. Metal dispersion and support effects on reaction rate and selectivity, Journal of Catalysis 137 (1) (1992) 212 – 224.
URL http://www.sciencedirect.com/science/article/pii/002195179290150G

[2] Design, synthesis, and use of cobalt-based Fischer-Tropsch synthesis catalysts , Applied Catalysis A: General 161 (12) (1997) 59 – 78.
URL http://www.sciencedirect.com/science/article/pii/S0926860X97001865

[3] R. C. Reuel, C. H. Bartholomew, Effects of support and dispersion on the CO hydrogenation activity/selectivity properties of cobalt, Journal of Catalysis 85 (1) (1984) 78 – 88.
URL http://www.sciencedirect.com/science/article/pii/0021951784901118

[4] R. Riva, H. Miessner, R. Vitali, G. D. Piero, Metal-support interaction in Co/SiO_2 and Co/TiO_2, Applied Catalysis A: General 196 (1) (2000) 111 – 123.
URL http://www.sciencedirect.com/science/article/pii/S0926860X99004603

[5] L. Shi, J. Chen, K. Fang, Y. Sun, CH_3-modified $Co/Ru/SiO_2$ catalysts and the performances for Fischer-Tropsch synthesis, Fuel 87 (45) (2008) 521 – 526, the 9th China-Japan Symposium on Coal and {C1} Chemistry.
URL http://www.sciencedirect.com/science/article/pii/S0016236107001469

[6] L. Shi, D. LI, B. Hou, Y. Sun, Organic modification of SiO_2 and its influence on the properties of Co-based catalysts for Fischer-Tropsch synthesis, Chinese Journal of Catalysis 28 (11) (2007) 999 – 1002.
URL http://www.sciencedirect.com/science/article/pii/S1872206707600849

[7] L. Jia, L. Jia, D. Li, B. Hou, J. Wang, Y. Sun, Silylated Co/SBA-15 catalysts for Fischer-Tropsch synthesis, Journal of Solid State Chemistry 184 (3) (2011) 488 – 493.
URL http://www.sciencedirect.com/science/article/pii/S0022459610004561

[8] M. Ojeda, F. J. Prez-Alonso, P. Terreros, S. Rojas, T. Herranz, M. Lpez Granados, J. L. G. Fierro, Silylation of a Co/SiO_2 Catalyst. Characterization and Exploitation of the CO Hydrogenation Reaction, Langmuir 22 (7) (2006) 3131–3137, pMID: 16548568.
URL http://dx.doi.org/10.1021/la052980c

[9] E. Richard, S. Aruna, B. J. Basu, Superhydrophobic surfaces fabricated by surface modification of alumina particles, Applied Surface Science 258 (24) (2012) 10199–10204.

[10] W. Bao, F. Guo, H. Zou, S. Gan, X. Xu, K. Zheng, Synthesis of hydrophobic alumina aerogel with surface modification from oil shale ash, Powder Technology 249 (2013) 220–224.

[11] L. J. Jallo, M. Schoenitz, E. L. Dreizin, R. N. Dave, C. E. Johnson, The effect of surface modification of aluminum powder on its flowability, combustion and reactivity, Powder Technology 204 (1) (2010) 63–70.

[12] ExxonMobil, 2015 the outlook for energy: A view to 2040 (2014).

[13] M. E. Dry, The Fischer-Tropsch process: 1950-2000, Catalysis Today 71 (34) (2002) 227 – 241, Fischer-Tropsch synthesis on the eve of the {XXI} Century.
URL http://www.sciencedirect.com/science/article/pii/S0920586101004539

[14] J. Hu, F. Yu, Y. Lu, Application of Fischer-Tropsch synthesis in biomass to liquid conversion, Catalysts 2 (2) (2012) 303–326.

[15] A. Y. Khodakov, W. Chu, P. Fongarland, Advances in the development of novel cobalt Fischer-Tropsch catalysts for synthesis of long-chain hydrocarbons and clean fuels, Chemical Reviews 107 (5) (2007) 1692–1744.

[16] G. Jacobs, T. K. Das, Y. Zhang, J. Li, G. Racoillet, B. H. Davis, Fischer-Tropsch synthesis: support, loading, and promoter effects on the reducibility of cobalt catalysts, Applied Catalysis A: General 233 (12).
URL http://www.sciencedirect.com/science/article/pii/S0926860X02001953

[17] Y. Liu, H. Guo, L. Jia, Z. Ma, Y. Xiao, C. Chen, M. Xia, B. Hou, D. Li, Fischer-Tropsch synthesis over alumina-supported cobalt-based catalysts: Effect of support variables, Journal of Materials Science and Chemical Engineering 2 (12) (2014) 263 – 281.

[18] P. Dimitrova, D. Mehandjiev, Active surface of γ-Al_2O_3-supported Co_3O_4, Journal of Catalysis 145 (2) (1994) 356 – 363.
URL http://www.sciencedirect.com/science/article/pii/S002195178471044X

[19] J. A. Lapszewicz, H. J. Loeh, J. R. Chipperfield, The effect of catalyst porosity on methane selectivity in the Fischer-Tropsch reaction, J. Chem. Soc., Chem. Commun. (1993) 913–914.
URL http://dx.doi.org/10.1039/C39930000913

[20] R. Riva, H. Miessner, G. D. Piero, B. Rebours, M. Roy, Dispersion and reducibility of Co/SiO_2 and Co/TiO_2, in: F. F. A. V. A. Parmaliana, D. Sanfilippo, F. Arena (Eds.), Natural gas conversion V proceedings of the 5th international natural gas conversion symposium,, Vol. 119 of Studies in Surface Science and Catalysis, Elsevier, 1998, pp. 203 – 208.
URL http://www.sciencedirect.com/science/article/pii/S0167299198804321

[21] C. Aaserud, A.-M. Hilmen, E. Bergene, S. Eric, D. Schanke, A. Holmen, Hydrogenation of propene on cobalt Fischer-Tropsch catalysts, Catalysis Letters 94 (3-4) (2004) 171–176.
URL http://dx.doi.org/10.1023/B%3ACATL.0000020541.28174.c7

[22] W.-J. Wang, Y.-W. Chen, Influence of metal loading on the reducibility and hydrogenation activity of cobalt/alumina catalysts, Applied Catalysis 77 (2) (1991) 223 – 233.
URL http://www.sciencedirect.com/science/article/pii/0166983491800677

[23] A. Y. Khodakov, A. Griboval-Constant, R. Bechara, V. L. Zholobenko, Pore size effects in Fischer-Tropsch synthesis over cobalt-supported mesoporous silicas, Journal of Catalysis 206 (2) (2002) 230 – 241.
URL http://www.sciencedirect.com/science/article/pii/S0021951701934967

[24] M. Vo, D. Borgmann, G. Wedler, Characterization of alumina, silica, and titania supported cobalt catalysts, Journal of Catalysis 212 (1) (2002) 10 – 21.
URL http://www.sciencedirect.com/science/article/pii/S0021951702937395

[25] A. Saib, M. Claeys, E. van Steen, Silica supported cobalt Fischer-Tropsch catalysts: effect of pore diameter of support, Catalysis Today 71 (34) (2002) 395 – 402, Fischer-Tropsch synthesis on the eve of the {XXI} Century.
URL http://www.sciencedirect.com/science/article/pii/S0920586101004667

[26] S. Storster, Ø. Borg, E. Blekkan, A. Holmen, Study of the effect of water on Fischer-Tropsch synthesis over supported cobalt catalysts, Journal of Catalysis

231 (2) (2005) 405 – 419.
URL http://www.sciencedirect.com/science/article/pii/S002195170500059X

[27] D. Schanke, S. Eri, E. Rytter, C. Aaserud, A.-M. Hilmen, O. A. Lindvg, E. Bergene, A. Holmen, Fischer-Tropsch synthesis on cobalt catalysts supported on different aluminas, in: X. Bao, Y. Xu (Eds.), Natural Gas Conversion VII Proceedings of the 7th Natural Gas Conversion Symposium, Vol. 147 of Studies in Surface Science and Catalysis, Elsevier, 2004, pp. 301 – 306.
URL http://www.sciencedirect.com/science/article/pii/S0167299104800685

[28] S. Rane, Ø. Borg, J. Yang, E. Rytter, A. Holmen, Effect of alumina phases on hydrocarbon selectivity in Fischer-Tropsch synthesis, Applied Catalysis A: General 388 (1) (2010) 160–167.

[29] Ø. Borg, S. Storster, S. Eri, H. Wigum, E. Rytter, A. Holmen, The effect of water on the activity and selectivity for γ-alumina supported cobalt Fischer-Tropsch catalysts with different pore sizes, Catalysis Letters 107 (1-2) (2006) 95–102.
URL http://dx.doi.org/10.1007/s10562-005-9736-8

[30] Ø. Borg, P. D. Dietzel, A. I. Spjelkavik, E. Z. Tveten, J. C. Walmsley, S. Diplas, S. Eri, A. Holmen, E. Rytter, Fischer-Tropsch synthesis: cobalt particle size and support effects on intrinsic activity and product distribution, Journal of Catalysis 259 (2) (2008) 161–164.

[31] L. Wu, Y. Huang, Z. Wang, L. Liu, H. Xu, Fabrication of hydrophobic alumina aerogel monoliths by surface modification and ambient pressure drying, Applied Surface Science 256 (20) (2010) 5973–5977.

[32] Pearl GTL - an overview - Shell Global.
URL http://www.shell.com/global/aboutshell/major-projects-2/pearl/overview.html

[33] A. de Klerk, Fischer-Tropsch Refining, John Wiley & Sons, 2012.

[34] J. A. Moulijn, M. Makkee, A. E. Van Diepen, Chemical process technology, John Wiley & Sons, 2013.

[35] M. Dry, Chapter 3 - Chemical concepts used for engineering purposes, in: A. Steynberg, M. Dry (Eds.), Fischer-Tropsch Technology, Vol. 152 of Studies in Surface Science and Catalysis, Elsevier, 2004, pp. 196 – 257.
URL http://www.sciencedirect.com/science/article/pii/S0167299104804609

[36] A. de Klerk, E. Furimsky, Catalysis in the refining of Fischer-Tropsch Syncrude, no. 4, Royal Society of Chemistry, 2010.

[37] M. Dry, Chapter 7 - FT catalysts, in: A. Steynberg, M. Dry (Eds.), Fischer-Tropsch Technology, Vol. 152 of Studies in Surface Science and Catalysis, Elsevier, 2004, pp. 533 – 600.
URL http://www.sciencedirect.com/science/article/pii/S0167299104804646

[38] G. Ertl, Wiley InterScience (Online service), Handbook of heterogeneous catalysis, Wiley-VCH ; John Wiley, distributor], Weinheim; Chichester, 2008.
URL http://dx.doi.org/10.1002/9783527619474

[39] J. R. Ross, Heterogeneous Catalysis: Fundamentals and Applications, Elsevier, 2012.

[40] A. Boumaza, L. Favaro, J. Lédion, G. Sattonnay, J. Brubach, P. Berthet, A. Huntz, P. Roy, R. Tétot, Transition alumina phases induced by heat treatment of boehmite: an X-ray diffraction and infrared spectroscopy study, Journal of solid state chemistry 182 (5) (2009) 1171–1176.

[41] G. Busca, Chapter three - structural, surface, and catalytic properties of aluminas, Vol. 57 of Advances in Catalysis, Academic Press, 2014, pp. 319 – 404.
URL http://www.sciencedirect.com/science/article/pii/B9780128001271000035

[42] S. Kurta, Investigating active centers of industrial catalysts for the oxidative chlorination of ethylene on a γ-Al_2O_3 surface, Catalysis in Industry 3 (2) (2011) 136–143.

[43] S. Storsæter, B. Tøtdal, J. C. Walmsley, B. S. Tanem, A. Holmen, Characterization of alumina-, silica-, and titania-supported cobalt Fischer-Tropsch catalysts, Journal of Catalysis 236 (1) (2005) 139 – 152.
URL http://www.sciencedirect.com/science/article/pii/S0021951705003684

[44] Ø. Borg, N. Hammer, S. Eri, O. A. Lindvg, R. Myrstad, E. A. Blekkan, M. Rønning, E. Rytter, A. Holmen, Fischer-Tropsch synthesis over un-promoted and Re-promoted γ-Al_2O_3 supported cobalt catalysts with different pore sizes , Catalysis Today 142 (12) (2009) 70 – 77, selection of papers presented in Session 10, Natural Gas Conversion, at the Europacat {VIII} Conference, Turku (bo), Finland, August 26-31, 2007.
URL http://www.sciencedirect.com/science/article/pii/S0920586109000315

[45] J. Zhang, J. Chen, J. Ren, Y. Li, Y. Sun, Support effect of Co/Al_2O_3 catalysts for Fischer-Tropsch synthesis, Fuel 82 (5) (2003) 581 – 586.
URL http://www.sciencedirect.com/science/article/pii/S0016236102003319

[46] S. Rane, Ø. Borg, E. Rytter, A. Holmen, Relation between hydrocarbon selectivity and cobalt particle size for alumina supported cobalt Fischer-Tropsch catalysts, Applied Catalysis A: General 437 (2012) 10–17.

[47] E. Rytter, S. Eri, T. H. Skagseth, D. Schanke, E. Bergene, R. Myrstad, A. Lindvåg, Catalyst particle size of cobalt/rhenium on porous alumina and the effect on Fischer-Tropsch catalytic performance, Industrial & Engineering Chemistry Research 46 (26) (2007) 9032–9036.

[48] Y. Zhang, K. Hanayama, N. Tsubaki, The surface modification effects of silica support by organic solvents for Fischer-Tropsch synthesis catalysts, Catalysis Communications 7 (5) (2006) 251 – 254.
URL http://www.sciencedirect.com/science/article/pii/S156673670500261X

[49] J. Zhang, J. Chen, J. Ren, Y. Sun, Chemical treatment of γ-Al_2O_3 and its influence on the properties of co-based catalysts for Fischer-Tropsch synthesis, Applied Catalysis A: General 243 (1) (2003) 121 – 133.
URL http://www.sciencedirect.com/science/article/pii/S0926860X02005410

[50] Ø. Borg, S. Eri, E. A. Blekkan, S. Storster, H. Wigum, E. Rytter, A. Holmen, Fischer-Tropsch synthesis over γ-alumina-supported cobalt catalysts: Effect of support variables, Journal of Catalysis 248 (1) (2007) 89 – 100.
URL http://www.sciencedirect.com/science/article/pii/S0021951707001042

[51] E. F. Vansant, P. Van Der Voort, K. C. Vrancken, Characterization and chemical modification of the silica surface, Elsevier, 1995.

[52] G. Busca, The surface of transitional aluminas: A critical review, Catalysis Today 226 (2014) 2–13.

[53] J. P. Blitz, R. Murthy, D. E. Leyden, Studies of silylation of Cab-O-Sil with methoxymethylsilanes by diffuse reflectance FTIR spectroscopy, Journal of Colloid and Interface Science 121 (1) (1988) 63 – 69.
URL http://www.sciencedirect.com/science/article/pii/0021979788904080

[54] W. J. Eakins, Silanol groups on silica and their reactions with trimethyl chlorosilane and trimethysilanol, I&EC Product Research and Development 7 (1) (1968) 39–43.
URL http://dx.doi.org/10.1021/i360025a009

[55] J. Regalbuto, Catalyst preparation: Science and Engineering, CRC Press, 2006.

[56] J. W. Niemantsverdriet, Spectroscopy in Catalysis, John Wiley & Sons, 2007.

[57] J. M. Thomas, W. J. Thomas, Principles and Practice of Heterogeneous Catalysis, VCH, Weinheim ; New York, 1997.

[58] M. A. Vannice, W. H. Joyce, Kinetics of Catalytic Reactions, Vol. 134, Springer, 2005.

[59] F. Delannay, et al. (Eds.), Characterization of Heterogeneous Catalysts, no. v. 15 in Chemical industries, M. Dekker, New York, 1984.

[60] M. Rønning, N. E. Tsakoumis, A. Voronov, R. E. Johnsen, P. Norby, W. van Beek, Ø. Borg, E. Rytter, A. Holmen, Combined XRD and XANES studies of a Re-promoted Co/γ-Al_2O_3 catalyst at Fischer-Tropsch synthesis conditions, Catalysis Today 155 (3) (2010) 289–295.

[61] B. C. Smith, Fundamentals of Fourier Transform Infrared Spectroscopy, CRC press, 2011.

[62] P. Larkin, Infrared and Raman Spectroscopy; Principles and Spectral Interpretation, Elsevier, 2011.

[63] A. W. Coats, J. P. Redfern, Thermogravimetric analysis. a review, Analyst 88 (1963) 906–924.
URL http://dx.doi.org/10.1039/AN9638800906

[64] M. Boudart, Turnover rates in heterogeneous catalysis, Chemical reviews 95 (3) (1995) 661–666.

[65] H. M. McNair, J. M. Miller, Basic gas chromatography, John Wiley & Sons, 2011.

[66] F. Katasek, R. Clement, Basic gas chromatography-mass spectrometry: Principles and techniques (1990).

[67] E. Rytter, S. Eri, T. H. Skagseth, D. Schanke, E. Bergene, R. Myrstad, A. Lindvg, Catalyst particle size of cobalt/rhenium on porous alumina and the effect on Fischer-Tropsch catalytic performance, Industrial & Engineering Chemistry Research 46 (26) (2007) 9032–9036.
URL http://dx.doi.org/10.1021/ie071136+

[68] I. Chorkendorff, J. W. Niemantsverdriet, Concepts of Modern Catalysis and Kinetics, John Wiley & Sons, 2006.

[69] N. Kourkoumelis, Powdll, a reusable .net component for interconverting powder diffraction data: Recent developments, Powder Diffraction 28 (02) (2013) 137–148.

[70] G. S. Pawley, Unit-cell refinement from powder diffraction scans, Journal of Applied Crystallography 14 (6) (1981) 357–361.
URL http://dx.doi.org/10.1107/S0021889881009618

[71] M. Wojdyr, *Fityk*: a general-purpose peak fitting program, Journal of Applied Crystallography 43 (5 Part 1) (2010) 1126–1128.
URL http://dx.doi.org/10.1107/S0021889810030499

[72] M. Capel-Sanchez, L. Barrio, J. Campos-Martin, J. Fierro, Silylation and surface properties of chemically grafted hydrophobic silica, Journal of Colloid and Interface Science 277 (1) (2004) 146 – 153.
URL http://www.sciencedirect.com/science/article/pii/S0021979704004321

[73] Ø. Borg, M. Rønning, S. Stors, W. van Beek, A. Holmen, et al., Identification of cobalt species during temperature programmed reduction of Fischer-Tropsch catalysts, Studies in surface science and catalysis 163 (2007) 255–272.

[74] A. Khodakov, J. Lynch, D. Bazin, B. Rebours, N. Zanier, B. Moisson, P. Chaumette, Reducibility of cobalt species in silica-supported Fischer-Tropsch catalysts, Journal of Catalysis 168 (1) (1997) 16 – 25.
URL http://www.sciencedirect.com/science/article/pii/S0021951797915736

[75] Ø. Borg, N. Hammer, B. C. Enger, R. Myrstad, O. A. Lindvg, S. Eri, T. H. Skagseth, E. Rytter, Effect of biomass-derived synthesis gas impurity elements on cobalt Fischer-Tropsch catalyst performance including In-situ sulphur and nitrogen addition, Journal of Catalysis 279 (1) (2011) 163 – 173.
URL http://www.sciencedirect.com/science/article/pii/S0021951711000273

[76] G. L. Bezemer, J. H. Bitter, H. P. C. E. Kuipers, H. Oosterbeek, J. E. Holewijn, X. Xu, F. Kapteijn, A. J. van Dillen, K. P. de Jong, Cobalt particle size effects in the Fischer-Tropsch reaction studied with carbon nanofiber supported catalysts, Journal of the American Chemical Society 128 (12) (2006) 3956–3964, pMID: 16551103.
URL http://dx.doi.org/10.1021/ja058282w

[77] R. Myrstad, FT-rigg: apparatur og prosedyrer for 4-reaktors fixed bed rigg, Sintef Kjemi, 2009.

Appendix A

Risk Analysis

Risk evaluation performed for laboratory experiments is given in this appendix.

Material safety data sheets of chemicals and NTNU HSE handbook are the basis of this assessment. Risk analysis was performed in collaboration of supervisor. Appropriate safety measure were suggested for identified potential hazards.

NTNU	Hazardous activity identification process	Prepared by	Number	Date
		HSE section	HMSRV2601	22/03/2011
		Approved by	Page	Replaces
HSE		The Rector		01/12/2006

Unit: *(Department)* ***Kjemisk prosessteknologi*** **Date:** 15/01/2015

Line manager: ***Edd Blekkan***

Participants in the identification process (incl. function)**:** Ata ul Rauf Salman (Master student), Nikolaos Tsakoumis (Co-Supervisor), Magnus Rønning (Supervisor)
(supervisor, student, co-supervisor, others)

Short description of the main activity/main process: Master project for student Ata ul Rauf Salman. Project title: Surface Modified gamma-alumina support for Fischer Tropsch

Is the project work purely theoretical? (YES/NO) No *Answer "YES" implies that* ***supervisor is assured that no activities requiring risk assessment are involved in the work****. If YES, briefly describe the activities below. The risk assessment form need not be filled out.*

Signatures: *Responsible supervisor:* _____ *Student:* _____

ID nr.	Activity/process	Respons-ible person	Existing documentation	Existing safety measures	Laws, regulations etc.	Comment
1	Use of pressurized / flamable gases (H_2)	Master student: Ata ul Rauf Salman		Use of required protective equipment: Gas alarms, transportation trolley, safety glasses, gas detector.		Gas bottle pressure: 200-220bar; Operating pressure: 1-25bar; Flamable/explosive gasses
2	Use of pressurized poisonous gases (Syngas)	Master student: Ata ul Rauf Salman		Use of required protective equipment: Gas alarms, transportation trolley, safety glasses, gas detector.		220bar; Operating pressure: 1-25bar; Flamable/explosive/pressurised gasses
3	Use of pressurized non-toxic/non-flamable gases(CO_2, O_2, Ar etc.)	Master student: Ata ul Rauf Salman		Use of required protective equipment: Gas alarms, transportation trolley, safety glasses, gas detector.		Gas bottle pressure: 200-220bar; Operating pressure: 1-25bar;
4	Use of ethanol/acetone	Master student: Ata ul Rauf Salman		Use of required protective equipment: Safety gloves, Safety Glasses		

5	Use of chemicals Toxic Chemicals, Chlorotrimethylsilane//Methoxytrimethylsilane/Dichlorodimethylsilane/Chlorodimethyloctylsilane/Methoxydimethyloctylsilane/Trichloroctylsilane/n-hexane/Perhanic Acid/Cobalt Nitrate Hexahydrate	Master student: Ata ul Rauf Salman		Use of required protective equipment: Safety vinyl gloves, Safety Glasses, Safety Mask		Use and Handling of chemimcals inside vacuum cupboard
6	Leak test and maintainance of FT-Rig	Master student: Ata ul Rauf Salman		Use of required protective equipment: Gas alarms, transportation trolley, safety glasses, gas detector.		Working pressure: 1-25bar; Flamable gases; Poisonous gases;
7	Operating FT-Rig	Master student: Ata ul Rauf Salman		Use of required protective equipment: Gas alarms, transportation trolley, safety glasses, gas detector.		Following standard operating procedure, Continuous Vigiliance, All gas/fire alarms are active

NTNU	Risk assessment	Prepared by	Nummer	Date
		HSE section	HMSRV2603	04/02/2011
		Approved by	Page	Replaces
HMS /KS		The Rector		09/02/2010

Unit: *(Institute)* ***Kjemisk prosessteknologi*** **Date:** 15/01/2015

Line manager: ***Edd Blekkan***

Participants in the identification process (incl. function): *Ata ul Rauf Salman (Master student), Nikolaos Tsakoumis (Co-Supervisor), Magnus Rønning (Supervisor)*

(supervisor, student, co-supervisor, others)

Risk assessment of: Master project for student Ata ul Rauf Salman. Project title: Surface Modified gamma-alumina support for Fischer Tropsch

Signatures: *Responsible supervisor:* _____ *Student:* _____

ID nr.	Activity from the identification process form	Potential undesirable incident/strain	Likeli-hood:	Consequence:				Risk value (human)	Comments/status Suggested measures
			(1-5)	Human (A-E)	Enviroment (A-E)	Economy/ material (A-E)			
1	Use of pressurized / flamable gases (H2)	Minor gas leakages	2	B	A	A		B2	
1	Use of pressurized / flamable gases (H2)	Larger gas leakages/Explosion/Fire	1	C	A	C		C1	
2	Use of pressurized poisonous gases (Syngas)	Small gas leakages/Inhalation	2	B	A	A		B2	
2	Use of pressurized poisonous gases (Syngas)	Larger gas leakages/Inhalation	1	C	C	C		C1	

3	Use of pressurized non-toxic/non-flamable gases(CO2, O2, Ar etc.)	Gas leakages	2	B	A	A		**B2**	
4	Use of ethanol/acetone	Spills/Chemical exposure	2	A	A	A		**A2**	
5	Use of chemicals Toxic Chemicals, Chlorotrimethylsilane//Methoxytrimethylsilane/Dichlorodimethylsilane/Chlorodimethyloctylsilane/Methoxydimethyloctylsilane/Trichloroctylsilane/n-hexane/Perhanic Acid/Cobalt Nitrate Hexahydrate	Spills/Chemical exposure	2	B	A	A		**B2**	
6	Leak test and maintainance of FT-Rig	Minor Gas leakages	5	A	A	A		**A5**	detector/Minor leakage occur and are checked in
7	Operating FT-Rig	Uncontrollable/Malfunction of controller or MFC	1	D	C	D		**D1**	

Risk value = Likelihood (1, 2 ...) x consequence (A, B ...). Risk value A1 means very low risk. Risk value E5 means very large and serious risk

Likelihood		Consequence					
Value	Criteria	Grading		Human	Environment	Economy/material	
1	**Minimal**: Once every 50 year or less	E	Very critical	May produce fatality/ies	Very prolonged, non-reversible damage	Shutdown of work >1 year.	
2	**Low**: Once every 10 years or less	D	Critical	Permanent injury, may produce serious health damage/sickness	Prolonged damage. Long recovery time.	Shutdown of work 0.5-1 year.	
3	**Medium**: Once a year or less	C	Dangerous	Serious personal injury	Minor damage. Long recovery time	Shutdown of work < 1 month	
4	**High**: Once a month or less	B	Relatively safe	Injury that requires medical treatment	Minor damage. Short recovery time	Shutdown of work < 1week	
5	**Very high**: Once a week	A	Safe	Injury that requires first aid	Insignificant damage. Short recovery time	Shutdown of work < 1day	

MATRIX FOR RISK ASSESSMENT

CONSEQUENCE	Very critical	E1	E2	E3	E4	E5
	Critical	D1	D2	D3	D4	D5
	Dangerous	C1	C2	C3	C4	C5
	Relatively safe	B1	B2	B3	B4	B5
	Safe	A1	A2	A3	A4	A5
		Minimal	Low	Medium	High	Very high
		LIKELIHOOD				

Explanation of the colors used in the risk matrix.

Color	Description
Red	Unacceptable risk. Safety measures must be implemented.
Yellow	Measures to reduce risk shall be considered.
Green	Acceptabel risk.

Appendix B

Calculation of amount of chemicals required for catalyst preparation

Fischer Tropsch catalyst with 20 wt% cobalt and 0.5 wt% rhenium on γ-alumina was prepared by one step incipient wetness impregnation of γ-Al_2O_3 supports with aqueous solutions of cobalt nitratehexahydrate, $Co(NO_3)_2.6H_2O$, and perrhenic acid, $HReO_4$. Important properties of precursor salts are summarised in table B.1

Table B.1: Chemical properties of metal precursors

Property	**Cobalt**	**Rhenium**
Chemical Formula	$CoN_2O_6.6H_2O$	$HReO_4$
Physical State	Solid	Solution
Molecular Weight	291.03 g/mole	251.21 g/mole
Density		2.16 g/mole
Purity		65-70 %

B.1 Catalyst preparation

The calculations to determine amount of precursor salts and de-ionised water needed for aqueous incipient impregnation of 10 g γ-Al_2O_3 support to get a metal loading of 20 wt % cobalt and 5 wt % rhenium are shown below and summarized in table B.2.

$$\begin{aligned} \text{Amount of alumina support} &= 10g \\ \text{Incipient wetness point} &= 12.8g \\ \text{Total mass of catalytic metals} &= \frac{10}{1-(0.2+0.005)} - 10 \end{aligned}$$

$$
\begin{aligned}
m_{metals} &= 2.5786g \\
\text{Total mass of cobalt } &= 2.5786 * \frac{0.2}{0.2 + 0.005} \\
m_{Co} &= 2.5157g \\
n_{Co} &= 2.5157/58.9331 \\
n_{Co} &= 0.04269 \text{ moles} \\
\text{Mass of cobalt precursor required} &= 0.04269 * 291.03 \\
m_{Co_{precursor}} &= 12.4233g \\
\text{Hydrated water in cobalt precursor} &= n_{Coprecursor} * 6 \\
\text{Hydrated water in cobalt precursor} &= 0.04269 * 6 \\
\text{Hydrated water in cobalt precursor} &= 0.2561\text{moles water} \\
\text{Hydrated water in cobalt precursor} &= 4.6098\text{g water} \\
\text{Total mass of rhenium } &= 2.5786 * \frac{0.005}{0.2 + 0.005} \\
m_{Re} &= 0.06289g \\
\text{Moles of rhenium } &= \frac{0.06289}{186.207} \\
n_{Re} &= 3.37 * 10^{-4} moles \\
m_{Re_{precursor}} &= 3.37 * 10^{-4} * 251.21 \\
&= 0.0848 gmoles \\
V_{Re_{precursor}} &= \frac{0.0848g}{2.16 \frac{g}{ml}} \\
V_{Re_{precursor}} &= 0.03926ml
\end{aligned}
$$

As precursor solution is 65-70% concentrated so taking average 67.5%

$$
\begin{aligned}
V_{Re_{precursor_{solution}}} &= \frac{0.03926}{0.675} \\
V_{Re_{precursor_{solution}}} &= 0.05816 \\
\text{Water present in rhenium precursor} &= V_{Re_{precursor_{solution}}} * 0.325 \\
\text{Water in rhenium precursor} &= 0.05816 * 0.325 \\
\text{Water in rhenium precursor} &= 0.0189 ml H_2O \\
\text{Water in rhenium precursor} &= 0.0189 g H_2O \\
\text{Total water in both precursor solutions} &= 4.6098 + 0.0189 \\
&= 4.6287 \\
\text{Amount of water needed} &= 12.8 - 4.6287 \\
&= 7.3713g
\end{aligned}
$$

Table B.2: Chemicals required to prepare Fischer Tropsch catalyst with 20 wt% Co and 0.5% Re

Component	**Amount**
Co Precursor	12.42 g
Re Precursor	0.058 ml
Water	7.371 g
γ-Al_2O_3	10.00 g

Appendix C

Incipient Wetness Point of Modified Supports

Hydrophobicity of surface modified supports was checked analytically by absorption of water. Trichloroctylsilane and methoxydimethyloctylsilane modified supports showed completely hydrophobic characteristics. All other supports absorbed water. Incipient wetness point of partially hydrophobic supports was found by dropwise addition of de-ionized water and reported in Table C.1.

Table C.1: Incipient wetness point of modified supports

Catalyst	**Incipient wetness point** [gH_2O/ g support]
(γ-Al_2O_3)	1.33
(γ-$Al_2O_3)_{Pr1}$	1.39
(γ-$Al_2O_3)_{Pr2}$	1.22
(γ-$Al_2O_3)_{Pr3}$	1.06
(γ-$Al_2O_3)_{Pr4}$	1.35
(γ-$Al_2O_3)_{Po1}$ [a]	Hydrophobic
(γ-$Al_2O_3)_{Po2}$ [a]	Hydrophobic

[a] Completely hydrophobic behavior.

Appendix D

Calculations for Amount of Chemicals Required for Surface Modification

Surface modification of the Fischer Tropsch Catalyst was carried out by immersing the sample in 100 ml of 1 % v/v solution of silane/n-hexane at 50^{o}C for 24 hours while continuously stirring. The sample was then washed with hexane and centrifuged three times to wash off unreacted silane and hexane. Important properties of the modification chemicals are given in table D.1.

Table D.1: Properties of the chemicals used in surface modification

Silane	Concentration	Mol. Weight	Boiling point
Methoxytrimethylsilane	99	104.22	57-58
Methoxydimethyloctylsilane	98	202.41	221-233
Chlorotrimethylsilane	99	108.64	57
Chlorodimethyloctylsilane	97	206.83	222-225
Dichlorodimethylsilane	99.5	129.06	70
Trichloroctylsilane	97	247.67	233
n-hexane	95	86.18	68

D.1 Calculation for preparation 1 vol% silane/n-hexane solution

Amount of chemicals required to prepare 1 vol% methoxydimethyloctylsilane/n-hexane solution are determined by following procedure.

$$\begin{aligned} \text{Methoxydimethyloctylsilane Needed} &= \frac{1}{100} * 100 \\ &= 1ml \end{aligned}$$

As methoxydimethyloctylsilane is 98% concentrated so

$$\begin{aligned} \text{Methoxydimethyloctylsilane solution needed} &= \frac{1}{0.98} \\ &= 1.020ml \\ \text{n-hexane needed} &= 100 - 1.020 \\ &= 98.98ml \end{aligned}$$

As n-hexane is 95% concentrated, therefore

$$\begin{aligned} \text{n-hexane solution needed} &= \frac{98.98}{0.95} \\ &= 104.1894ml \end{aligned}$$

Similar procedure is adopted to find out the amount of different silanes required to surface modification.

Appendix E

Calculation of Rate of Reaction and Site-Time Yield

The calculations to determine Site Time yield reported in activity measurement in section are presented in this appendix. All the data required and calculations are summarized in table. The sample calculations for the Site Time Yield calculations of reference catalyst are shown below.
Observed rate of reaction is calculated by equation E.1

$$r_{CO} = \frac{GHSV}{V_m}.X_{CO}.x_{CO} \tag{E.1}$$

where r_{CO} is the observed rate of reaction, V_m is the molar volume = 22400 cm^3/mol, X_{CO} is the CO conversion and x_{CO} is the CO mole fraction in feed.

$$\begin{aligned} r_{CO} &= \frac{14921}{22400} * 0.269 * 0.313 \\ &= 0.0560 molCO/g_{cat}h \end{aligned}$$

STY is calulated by using equation E.2. Where M is the molecular weight of the active metal, cobalt in this case, w_m is the weight fraction of active metal, and D is the dispersion.

$$STY = \frac{r_{CO}.M}{w_m.D} \tag{E.2}$$

$$= \frac{0.0560 * 58.9}{0.20 * 0.07588}.\frac{1}{3600}$$

$$= 0.0604 s^{-}1 \tag{E.3}$$

Appendix F

Process Flow Diagram of Fischer Tropsch Rig

Process flow diagram of Fischer-Tropsch rig used for the activity and selectivity measurement of the catalysts sample is given in this appendix. The figure is adopted from Fischer-Tropsch Rig Manual written by Rune Myrstad [77].

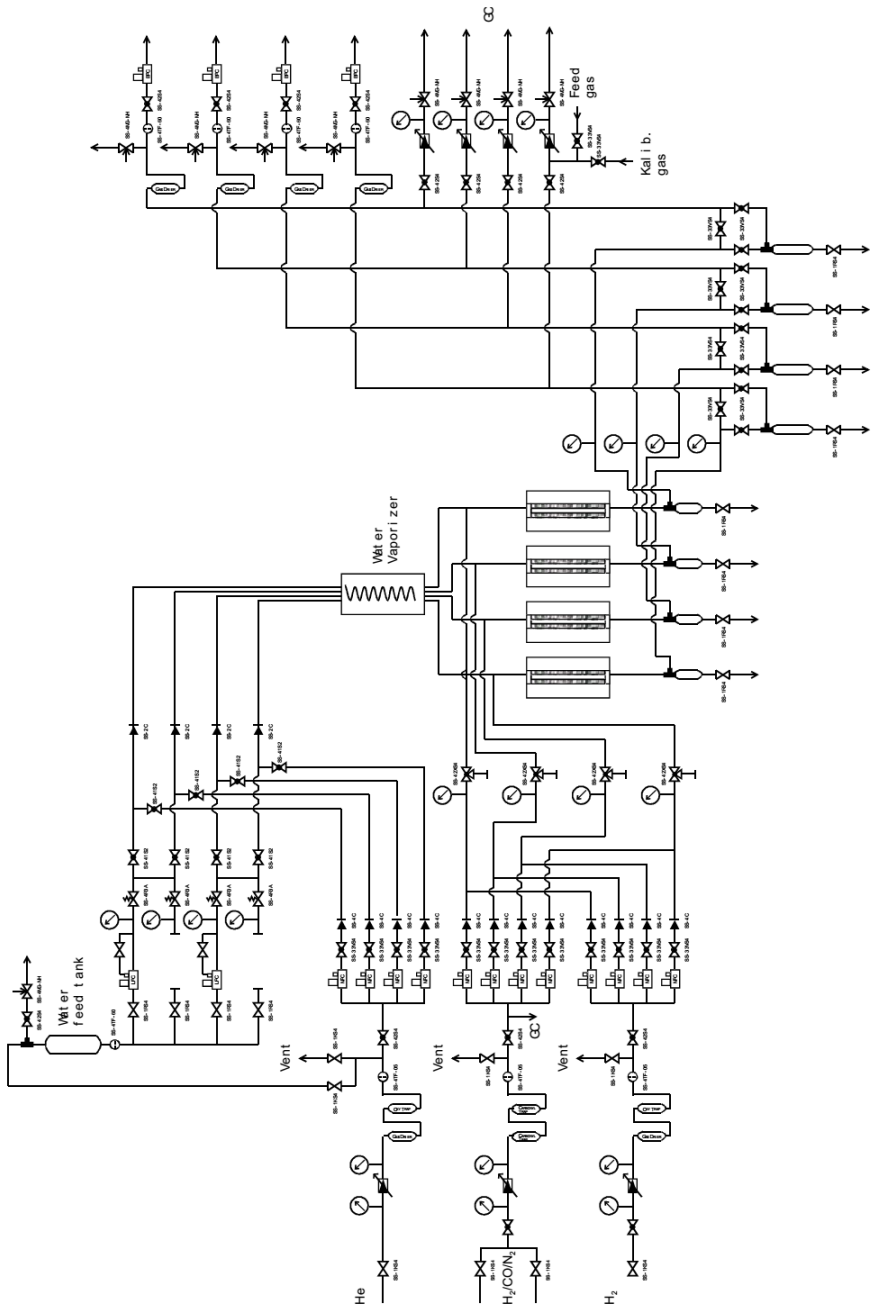

Figure F.1: Process flow diagram of the Fischer Tropsch rig, adopted from Myrstad [77]

Appendix G

TGA Mass Loss

Mass loss of modified supports and catalysts during TGA are given in this section.

Table G.1: Mass Loss of pre-modified supports from TGA

Support	**Mass Loss [%]**		
	30-150^oC	**150-800** ^oC	**Total (30-800** ^oC**)**
(γ-Al_2O_3)	2.67	2.89	5.57
(γ-Al_2O_3)$_{Pr1}$	1.81	4.00	5.81
(γ-Al_2O_3)$_{Pr2}$	3.08	4.94	8.02
(γ-Al_2O_3)$_{Pr3}$	2.50	4.78	7.28
(γ-Al_2O_3)$_{Pr4}$	2.62	5.04	7.66

Table G.2: Mass Loss of surface modified catalysts from TGA

Catalyst	**Mass Loss (%)**		
	30-150 ^oC	**150-800** ^oC	**30-800** ^oC
Co/γ-Al_2O_3	1.81	2.65	4.46
Co/(γ-Al_2O_3)$_{Pr1}$	2.55	4.14	6.69
Co/(γ-Al_2O_3)$_{Pr2}$	2.67	4.68	7.35
Co/(γ-Al_2O_3)$_{Pr3}$	0.76	3.49	4.24
Co/(γ-Al_2O_3)$_{Pr4}$	1.80	3.89	5.68
Co/(γ-Al_2O_3)$_{Po1}$	1.19	5.30	6.49
Co/(γ-Al_2O_3)$_{Po2}$	0.91	8.68	9.59

Table G.3: Relation between dispersion, cobalt crystallite size and Mass loss of catalyst during TGA

Catalyst	**Dispersion** [a] **[%]**	**Co^o Particulate Size [nm]**	**TGA Mass Loss [%]**
Co/s-(γ-Al_2O_3)$_{TMCS}$	2.33	6.90	7.35
Co/s-(γ-Al_2O_3)$_{DMOCS}$	3.49	8.60	5.68
Co/s-(γ-Al_2O_3)$_{DMDCS}$	5.63	7.80	4.24